

1 Article

2 Reduction of wave overtopping and force impact at 3 harbor quays due to very oblique waves

4 Sebastian Dan^{1,*}, Corrado Altomare^{1,2}, Tomohiro Suzuki^{1,3}, Tim Spiesschaert¹, Toon Verwaest¹

5 ¹ Flanders Hydraulics Research, Berchemlei 115, 2140 Antwerp, Belgium;
6 sebastian.dan@mow.vlaanderen.be, tomohiro.suzuki@mow.vlaanderen.be;
7 tim.spiesschaert@mow.vlaanderen.be; toon.verwaest@mow.vlaanderen.be

8 ² Universitat Politècnica de Catalunya – BarcelonaTech (UPC), 08034 Barcelona, Spain;
9 corrado.altomare@upc.edu

10 ³ Faculty of Civil Engineering and Geosciences, Delft University of Technology, Stevinweg 1, 2628, CN Delft,
11 the Netherlands

12 * Correspondence: sebastian.dan@mow.vlaanderen.be

13 Received: date; Accepted: date; Published: date

14 **Abstract:** Physical model experiments have been conducted in a wave tank at Flanders Hydraulics
15 Research, Antwerp to characterize the wave overtopping and impact force on vertical quay walls and
16 sloping sea dike (1:2.5) under very oblique wave attack (angle between 45° and 80°). This study was
17 triggered by the scarce scientific literature on the overtopping and force reduction due to very oblique
18 waves since large reduction is expected for both when compared with the perpendicular wave attack.
19 The study aimed to compare the results from the experimental tests with formulas derived from
20 previous experiments and applicable to a Belgian harbors generic case. The influence of storm return
21 walls and crest berm width on top of the dikes has been analyzed in combination with the wave
22 obliqueness. The results indicate significant reduction of the overtopping due to very oblique waves
23 and new reduction coefficients have been proposed. When compared with formulas from previous
24 studies [1] indicate the best fit for the overtopping reduction. Position of the storm return wall respect
25 to the quay edge rather than its height was found to be more important for preventing wave induced
26 overtopping. The force reduction is up to approximately 50% for the oblique waves with respect to
27 the perpendicular wave impact and reduction coefficients were proposed for two different
28 configurations a sea dike and vertical quay wall, respectively.

29 **Keywords:** Overtopping reduction, force reduction, oblique waves, storm return wall, EurOtop
30 manual.

31

32 1. Introduction

33 Densely populated coastal zones with very low freeboards are common worldwide (e.g.
34 Belgium, The Netherlands, Vietnam). Often the flood protection is provided in these zone by the
35 sandy beaches, but when it is insufficient or in the case of harbors the most common solution is the
36 storm walls construction. A storm wall is located on top of the crest of a quay or a dike at a certain
37 distance from the seaward edge of the crest, providing additional protection against the overtopping
38 waves. During each overtopping event, the waves run up in form of a bore along its crests before
39 reaching the wall. Usually, this flow is turbulent and its velocity is decreased along the crest width.

40 Consequently, the distance between the edge of the structure and the storm wall is important because
 41 it characterizes the wave impact on the storm wall and overtopping over the storm wall.

42 Typically, the waves' angle is assumed to be perpendicular or at an angle lower than 45° with
 43 respect to the quay's normal. However, when the harbor opening is orientated against the main wave
 44 direction very oblique waves can approach some of the harbor quays and dikes. There are several
 45 formulas proposed for the overtopping computation under oblique wave attack. One of the most
 46 widely used is the European Overtopping Manual [2,3] which provides validated formulas to
 47 calculate the overtopping discharge for classical configurations (wave angles smaller than 45°). The
 48 overtopping is maximum for the perpendicular wave attack on a storm return wall, but for larger
 49 wave angles a reduction factor is applied to account for the overtopping discharge decrease.
 50 However, the EurOtop formula suggests to keep the obliqueness reduction factor constant for vertical
 51 structures and wave angles larger than 45°. Obviously, the overtopping discharge reduces with the
 52 increasing wave angle with respect to the structure normal, but the reduction for very large wave
 53 angles has not been fully investigated yet. A similar situation is for the case of the impact force
 54 reduction due to the large wave angle, but studies comprehensively analyzing this reduction are not
 55 currently available.

56 The mean wave overtopping is mainly a function of the relative freeboard and the relationship
 57 between the overtopping discharge and the freeboard is expressed through, in most of the cases, an
 58 exponential formula. Several reduction coefficients are used to account for effects induced by the
 59 presence of a berm, a storm return wall, the surface roughness and the wave obliqueness.

60 To investigate the overtopping reduction and impact force reduction for oblique waves a
 61 physical model was set-up at Flanders Hydraulics Research in Antwerp, Belgium. The present study
 62 has three main objectives. Firstly, to investigate overtopping induced by very oblique waves at quay
 63 harbors and to propose reliable reduction coefficients for the overtopping calculation. Secondly, to
 64 identify the influence on overtopping of a storm return wall placed on the quay at different positions
 65 and having variable heights. Thirdly, to evaluate the impact force reduction due wave obliqueness.

66 2. Overtopping and force reduction

67 2.1 Vertical quay

68 A series of formulations describe the overtopping reduction with the large incident wave angle.
 69 Most used are presented in [2], but significant contributions are given also in the studies of de [1,4,5].
 70 The overtopping reduction due to very oblique wave angles is usually limited to angles of 45° and
 71 for larger wave angles a constant value is proposed.

72 The most used approach is based on the equations and reduction factors as contained in the
 73 European Overtopping Manual [2] for non-impulsive conditions:

$$74 \quad \frac{q}{\sqrt{gH_{m0}^3}} = 0.04 \exp\left(-2.6 \frac{R_c}{H_{m0}\gamma_\beta}\right) \quad (1)$$

75 where q is the overtopping discharge per meter of width of the structure [m³/s/m], H_{m0} is the
 76 significant incident wave height, measured at the toe of the structure [m], R_c is the crest freeboard
 77 [m], γ_β is the reduction coefficient that considers the effects of the obliqueness [-].

78 The coefficient γ_β is expressed in EurOtop as:

$$79 \quad \gamma_\beta = 1 - 0.0062|\beta| \quad \text{for: } 0^\circ \leq \beta \leq 45^\circ \quad (2)$$

80 For wave angles larger than 45° a constant value of 0.72 is proposed in EurOtop [2].

81 The formulations contained in the EurOtop manual [2] assume that different regimes of non-
 82 breaking, impulsive breaking and broken waves may produce differences in the overtopping.
 83 Although the wave loadings on vertical walls by individual waves are certainly affected by the wave
 84 regime, it is not clear that the overtopping is affected in the same way. The overtopping discharge is
 85 a mean value where many non-breaking, breaking and broken waves can contribute in the same

86 wave train. Therefore Goda [1] proposed an equation for both non-impulsive and impulsive wave
 87 conditions:

$$88 \quad \frac{q}{\sqrt{gH_{mo}^3}} = \exp \left[- \left(A + B \frac{R_c}{H_{mo}} \frac{1}{\gamma_f \gamma_\beta} \right) \right] \quad (3)$$

89 The constants A and B can be estimated by:

$$94 \quad \left. \begin{aligned} A &= A_0 \tanh \left[b_1 \left(\frac{h_t}{H_{s,toe}} + c_1 \right) \right] \\ B &= B_0 \tanh \left[b_2 \left(\frac{h_t}{H_{s,toe}} + c_2 \right) \right] \end{aligned} \right\} \quad (4)$$

95 where h_t is the water depth at the toe of the dike and $H_{s,toe}$ is the incident wave height at the toe
 96 of the dike. The coefficients b_1, c_1, b_2, c_2 depend on the foreshore slope as summarized in Table 1.

97 **Table 1.** Optimum coefficient values of empirical formulas for intercept A and gradient coefficient B
 98 (Goda, 2009).

Seabed slope	Coefficient A			Coefficient B		
$\tan\theta$	A0	b1	c2	B0	b2	c2
1/10	3.6	1.4	0.1	2.3	0.6	0.8
1/20 – 1/1000	3.6	1.0	0.6	2.3	0.8	0.6

99 The coefficients A_0 and B_0 are calculated in function of the dike slope, $\cot \alpha_s$, and their value
 100 ranges between 0 and 7. The expression for the reduction factor for wave obliqueness has been
 101 estimated by Goda [1] as:
 102

$$103 \quad \gamma_\beta = 1 - 0.0096|\beta| + 0.000054\beta^2 \quad \text{for } 0^\circ \leq \beta \leq 80^\circ \quad (5)$$

104 2.2 Sloping dike

105 Several studies investigate the reduction in overtopping due to oblique waves [6,7], but two
 106 formulas from literature have been considered due to the similarity with the tests from the present
 107 study: EurOtop [2] (6) for non-breaking waves and van der Meer and Bruce [8] (8) which is an
 108 adaptation of the EurOtop formula.

$$109 \quad \frac{q}{\sqrt{gH_{mo}^3}} = 0.2 \exp \left(-2.6 \frac{R_c}{H_{mo}} \frac{1}{\gamma_f \gamma_\beta} \right) \quad (6)$$

110 in which the coefficient γ_β is expressed as:

$$111 \quad \gamma_\beta = 1 - 0.0033|\beta| \quad \text{for: } 0^\circ \leq \beta \leq 80^\circ \quad (7)$$

112 For wave angles larger than 80° a constant value of 0.736 is proposed.

113 The formula given by van der Meer and Bruce [8]:

$$114 \quad \frac{q}{\sqrt{gH_{mo}^3}} = 0.09 \exp \left(-1.5 \frac{R_c}{H_{mo}} \frac{1}{\gamma_f \gamma_\beta} \right)^{1.3} \quad (8)$$

115 in which γ_β is identical as in (7)

116 In all the cases γ_f has been assumed equal to 1 (smooth slope). Van Doorslaer et al. [9]) propose
 117 a reduction factor γ_{prom_v} to take into account the presence of a storm return wall on the top of the dike.
 118 This coefficient considers both the effect of the wall height and position. The values of γ_{prom_v} are
 119 calculated for each case based on the approach described in Van Doorslaer et al. [9].

$$120 \quad \frac{q}{\sqrt{gH_{mo}^3}} = 0.2 \exp \left(-2.3 \frac{R_c}{H_{mo}} \frac{1}{\gamma_f \gamma_\beta \gamma_{prom_v}} \right) \quad (9)$$

$$121 \quad \gamma_{prom_v} = 0.87 \gamma_{prom} \gamma_v \quad (10)$$

122 where γ_{prom} and γ_v are the individual reduction factors to consider the effects respectively of the
 123 promenade and of the storm wall. The promenade reduction factor γ_{prom} is expressed as:

$$124 \quad \gamma_{prom} = 1 - 0.47 B/L_{m-1,0} \quad (11)$$

125 where B is the width of the promenade and $L_{m-1,0}$ is the spectral wave length calculated using the
 126 spectral period in deep waters $T_{m-1,0} = m-1/m0$.

127 The reduction factor γ_v for the presence of a storm return wall is expressed in Van Doorslaer et
 128 al. [9] in function of the wall height (h_{wall}) and freeboard (R_c) as follows:

$$129 \quad \gamma_v = \begin{cases} \exp(-0.56 h_{wall}/R_c) \\ 0.5 \end{cases} \quad \text{for} \quad \begin{cases} h_{wall}/R_c < 1.24 \\ h_{wall}/R_c \geq 1.24 \end{cases} \quad (12)$$

130 **2.3 Force reduction**

131 There is scarce information regarding the impact forces on a storm wall in case of wave
 132 overtopping by oblique waves. However, the study of Van Doorslaer et al. [10] performed at UPC
 133 Barcelona, used configurations similar to those tested in the present study. Two structures were
 134 tested in the wave flume (scale 1:6): a vertical quay wall and a dike with a smooth slope. The storm
 135 wall was 1.20 m high (prototype value) and located at 10.14 m (prototype value) behind the edge of
 136 the crest. Three water levels were used resulting in freeboard R_c from the still water level to the top
 137 of the storm wall of 3.18 m, 2.22 m and 1.20 m (prototype values). The irregular waves had a
 138 Jonswap wave spectrum ($\gamma = 3.3$). The significant wave height H_{m0} ranged from 0.78 m to 3.00 m
 139 (prototype values), the wave period T_p is either 7.00 s or 10.00 s. The experiments were carried out in
 140 two dimensional conditions with perpendicular waves (no wave obliqueness). The authors proposed
 141 a new formula to evaluate the wave force on a storm wall, both for quay walls and sea dikes. The
 142 formula can be expressed as follows:

$$143 \quad F_{1/250} = a \rho g R_c^2 \exp\left(-b \frac{R_c}{H_{m0}}\right) \quad (13)$$

144 where $F_{1/250}$ is the average force of the highest 1/250 waves. The coefficients a and b (Table 2) are
 145 derived from a non-linear regression analysis and they are considered as the mean value of normally
 146 distributed variables. Under this hypothesis, the relative standard deviation ($\sigma' = \sigma/\mu$) was calculated
 147 for each coefficient and is reported in Table 2 between brackets.

148 **Table 2.** Coefficients a and b in equation (13) for different geometries.

Geometry	a	b
Dike	8.31 (0.22)	2.45 (0.07)
Quay	18.27 (0.23)	3.99 (0.06)
All	5.96 (0.23)	2.42 (0.09)

149 **3. Methods and instrumentation**

150 Investigation of the overtopping reduction required a physical model sufficiently large to
 151 observe the alongshore variation and to accommodate the collection of the overtopped volumes,
 152 respectively. However, this structure was not firm enough to prevent vibrations which can severely
 153 alter the impacting forces measurements. Therefore, it was decided to build two different structures,
 154 first for the overtopping reduction and second for force reduction due to the wave obliqueness. The
 155 structural layout and hydraulic boundary conditions were assumed based on real conditions from
 156 the Belgian harbors. However, the model geometries do not represent one specific quay or dike, but
 157 it was selected in such way that the results might be extended to other similar structures. The

158 experiments were carried out in the wave tank at Flanders Hydraulics Research (dimensions 17.50m
159 x 12.20m x 0.45m), equipped with a piston-type wave generator. The wave generator has a width of
160 12 m and generates long-crested waves. Both regular and irregular wave patterns can be generated
161 at different angles of wave incidence ranging between -22.5° and 22.5° with respect to the center line
162 of the wave tank.

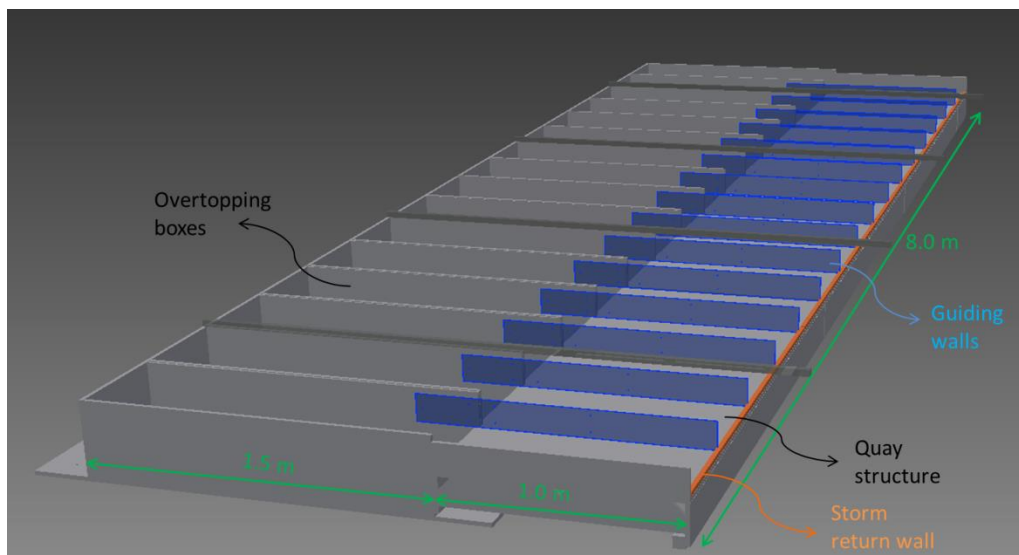
163 Two sets of wave directions were used in the experimental campaign conducted at FHR: the first
164 set contains the wave directions 0° and 45° , used to validate the results of the FHR experiments
165 against previous experiments and existing formulas; the second set contains wave directions 60° , 70°
166 and 80° , used to investigate larger angles. Similar configuration tests from CLASH database [11]
167 were used to compare and validate the tests from the present study.

168 3.1. Model settings of overtopping tests

169 The first physical model was designed to study very oblique wave attacks and overtopping flows
170 onto vertical quays and sloping dikes with storm return walls. As the wave height can variate along
171 the structure, a smaller scale was necessary to accommodate a model following the general prototype
172 conditions. However, the scale cannot be smaller than 1:50 because some wave height scenarios
173 would be smaller than 3 cm affected by the surface tension and thus altering the reproduction of the
174 prototype conditions [12]. After the scale has been evaluated and following Froude's law the model
175 scale was decided for 1:50. For vertical walls, tests in large scale flumes and field measurements have
176 demonstrated that results of overtopping discharge in small scale laboratory studies may be securely
177 scaled up to full scale under impulsive and non-impulsive conditions. Only the wind effects are not
178 considered and may cause a significant difference (further details see [2]). For dikes the evaluation of
179 scale effects is based on the approach of Schüttrumpf and Oumeraci [13]. Calculation of the Reynolds-
180 number and its comparison with the critical value demonstrated that scale effects are negligible. A
181 minimum distance between the wave maker and the structure equal to two wave lengths was kept
182 for every configuration and wave dampers were placed around the basin to absorb the reflected
183 waves. Considering the limitations, it was decided to build a laminated wooden structure of 8 m long
184 and 1 m wide. Attached to this structure, there are 16 boxes (1.5 m long, 0.48 m wide and 0.18 m
185 deep), built from the same material, designed to collect the overtopping water during the experiment
186 (**Error! Reference source not found.**).

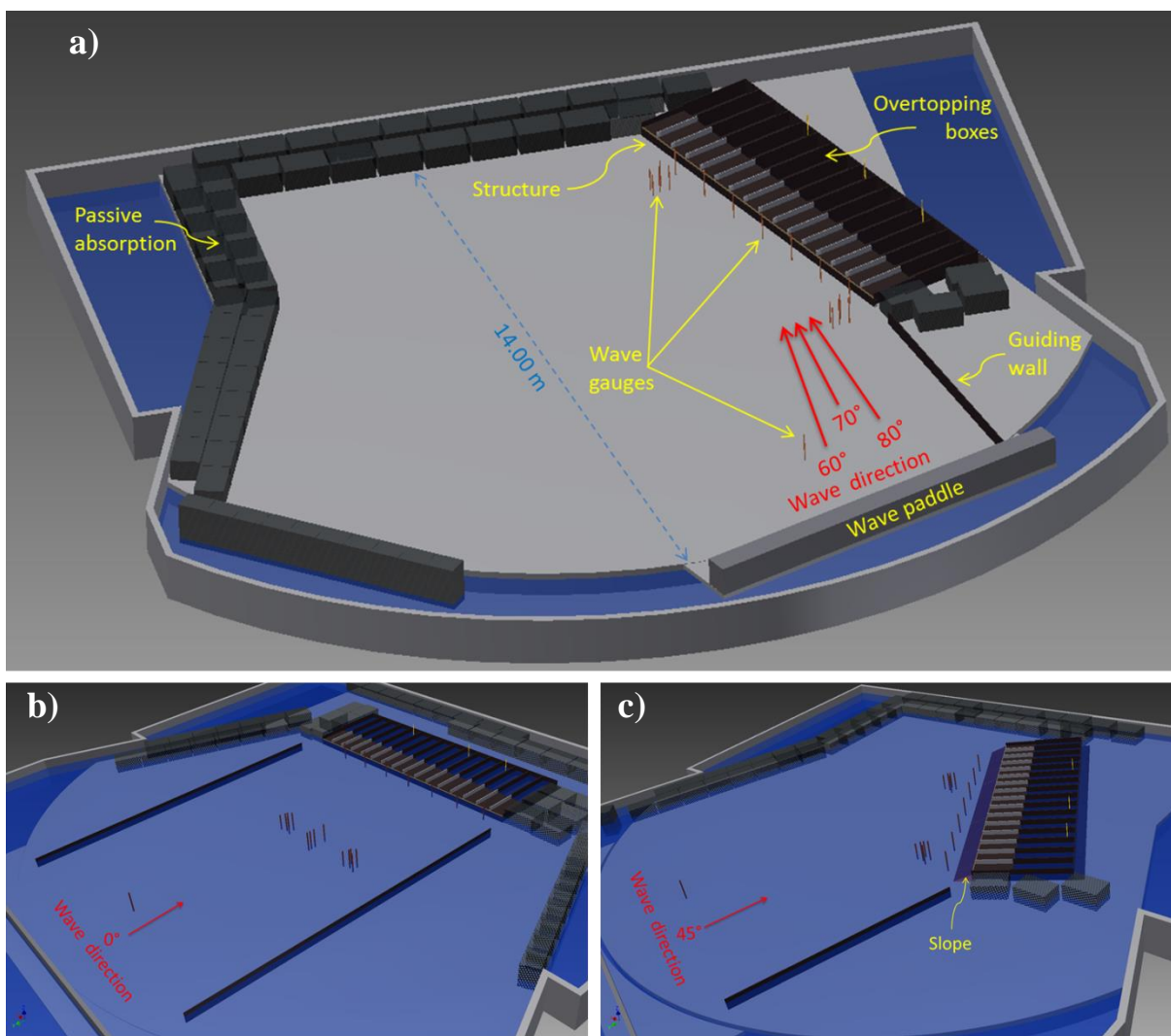
187 Two positions of this structure in the basin were foreseen. Firstly, the structure was mounted in the
188 central down part of the basin for the 0° wave direction (**Error! Reference source not found.**, b).
189 Secondly, the structure was moved towards the down left corner to optimize the distance to the wave
190 maker, but also to allow simulation of the wave directions between 45° and 80° just by moving the
191 wave paddle and keep the structure in the same position (**Error! Reference source not found.**, a and
192 c).

193



194
195

Figure 1. The structure used during the experiment.

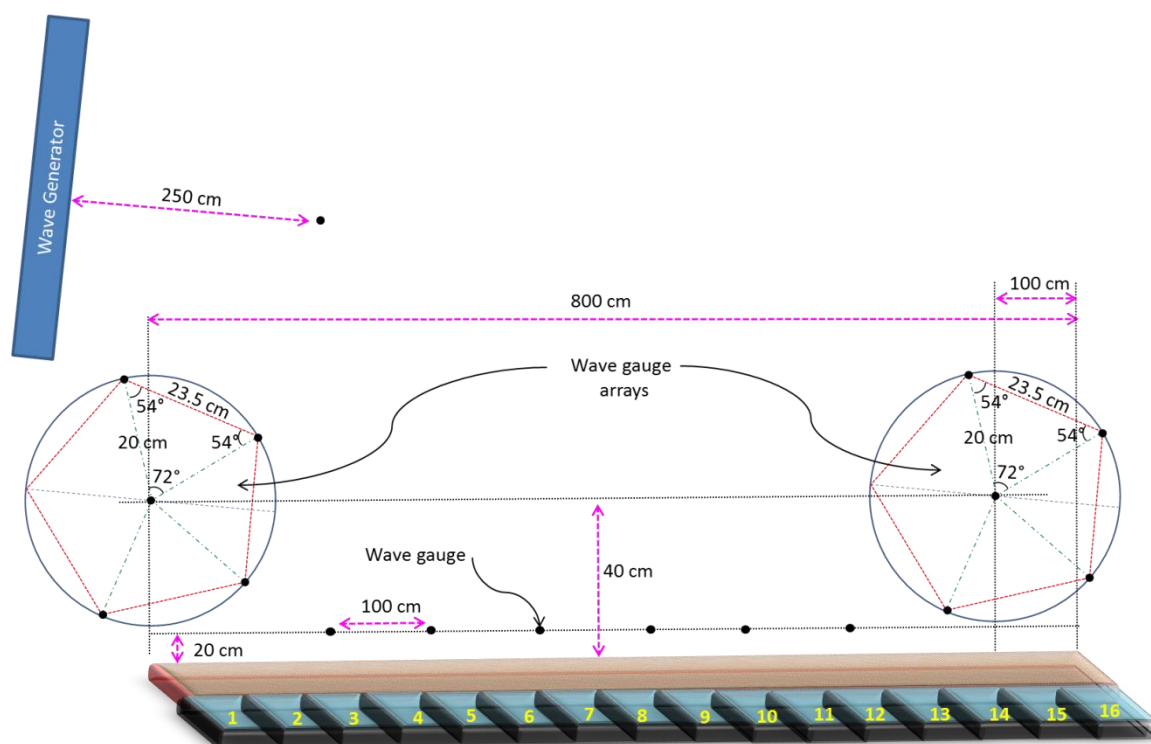


196
197
198

Figure 2. The position of the structure in the wave basin during experiments.

3.1.1. Instrumentation

199 A number of 17 wave gauges (resistance type) were used to measure the wave characteristics
 200 (height, period and direction). One wave gauge is permanently situated in front of the wave maker
 201 to verify the generated waves. Two wave gauges arrays have been built, each consisting of five wave
 202 gauges: these wave gauges are located in such way that a directional spectral analysis can be
 203 performed. The incident wave height has been measured using these two 3D-arrays. The WaveLab
 204 software (version 3.39, [14]) which utilizes the Bayesian Directional spectrum estimation method
 205 (BDM) [15], has been used for the analysis. Using this method, the user generally indicates a circular
 206 sector around the expected incident and reflected wave direction, so the analysis will be limited to
 207 this sector. It is possible to select a very narrow circular sector, excluding from the wave analysis
 208 directions too far from the main one. Alternatively, it also possible to select $\pm 90^\circ$ around the main
 209 direction, so the entire 360° will be covered from the analysis. In this study, the analysis for the
 210 perpendicular wave case attack used $\pm 30^\circ$ around the main expected directions (0° for the incident
 211 and 180° for the reflected waves respectively). Hence spurious transversal effects were removed from
 212 the results. Differently, for the oblique wave cases, it has been preferred to extend the analysis to the
 213 entire 360° , because in such case the main reflected direction can be presumed, but the effects on wave
 214 re-reflection on the sides of the basin (even though passive absorption was installed) has to be
 215 checked. The rest of the six wave gauges were mounted equidistantly, in the proximity of the
 216 structure to provide information about the total wave height variation along the structure. This
 217 instrument setup was used for all the wave directions, but some minor changes in distances and
 218 positions have been made for each wave direction (**Error! Reference source not found.**). On every
 219 overtopping box a mechanical reader for the water level was installed to measure the accumulated
 220 volume.



221
 222 **Figure 3.** Example of instrument distribution in the basin for the wave angle 80° (not to scale).

223 3.1.2. Test programme

224 The total number of tests was 377 covering a wide range of wave conditions and structure
 225 configurations (Table 3). The wave angle is defined as the angle between the wave direction and the
 226 line normal to the quay structure so that 0° defines perpendicular wave attack. For the majority of
 227 the wave angles both vertical and sloping dike configuration was used. In all the tests long-crested
 228 waves were generated. The water level has been varied around the crest level: the defined “dike
 229 freeboard” (R_c) assumes from negative (i.e. Still Water Level, SWL, above the dike crest) to positive
 230 values (SWL below the dike crest). Three different wall heights have been used (0 m, 1 m and 2 m in
 231 prototype scale). The wall elevation with respect to the SWL defines the crest freeboard R_c . Tests with
 232 no reliable measured wave conditions, zero overtopping and water volumes exceeding the boxes’
 233 volume, as well as preliminary tests to set-up the model have been excluded from further analyses.

234 **Table 3.** Summary of the test conditions for overtopping reduction.

Total no. of tests	Used for analyses	Vertical quay	Sloping dike (1:2.5)	
377	230	191	39	
Wave directions	Wave height (H_{m0})	Wave period (T_p)	Crest freeboard (R_c)	Storm return wall position
0°, 45°, 60°, 70°, 80°	0.96 to 3.39 m	5.1 to 12.6 s	0 to 2.75 m	0 to 50 m

235 The overtopping discharge per each overtopping box and the measured total wave height along
 236 the structure were analysed. In most of the tests, the overtopping boxes of both sides (from 0 to 1m
 237 and from 7÷7.5 to 8m) were not included in the calculation to avoid errors generated by model
 238 boundary effects. The calculation of the mean overtopping discharge starting from the measured
 239 overtopping volume follows geometrical rules as:

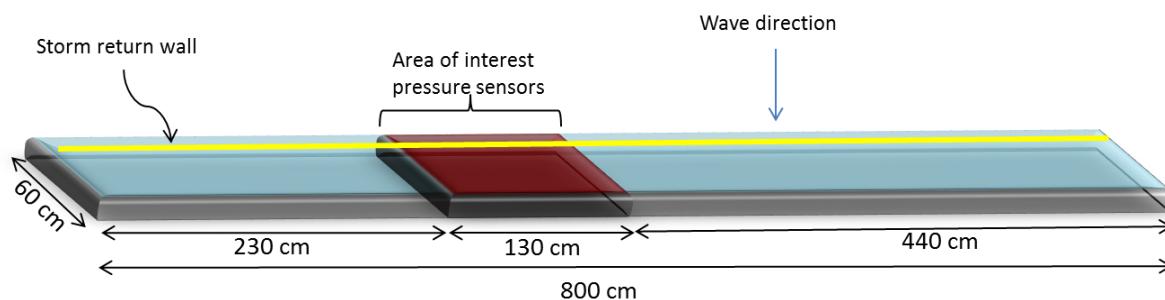
- 240 - For each test the berm length has been calculated as a distance between the edge of the quay
 241 (sea dike) and the crown wall.
- 242 - For each angle the projection of the berm length has been measured on the wave direction:
 243 this is the effective berm length that the wave has to run before reaching the wall.
- 244 - To calculate the mean overtopping for the entire quay some buffer zones at both edges of the
 245 structure have been skipped (where possible model effects are noticed). For instance, in the
 246 case with no crown wall or crown wall on the quay edge, the entire quay length (8 m) has
 247 been considered excluding the two overtopping boxes situated at the edges of the structure.
- 248 - It has been verified on video recordings that the peaks in the overtopping volume are not
 249 due to model effects (boundary reflection), but they are due to the wave attack.

250 **3.2. Model settings of force test**

251 The model built to investigate the reduction of the wave impact forces was very similar with
 252 the one for the overtopping reduction with the same 1:50 scale reduction. The structure (**Error!**
 253 **Reference source not found.**) had a length of 8 m, a width of 0.6 m and a height of 0.2 m. Based on
 254 the distribution of the largest wave heights and largest overtopping volumes along the structure an
 255 area of interest was selected approximately in the structure’s centre, where four force sensors
 256 (Tension Compression Load Cells, Model 641) were placed to record the time series of the wave

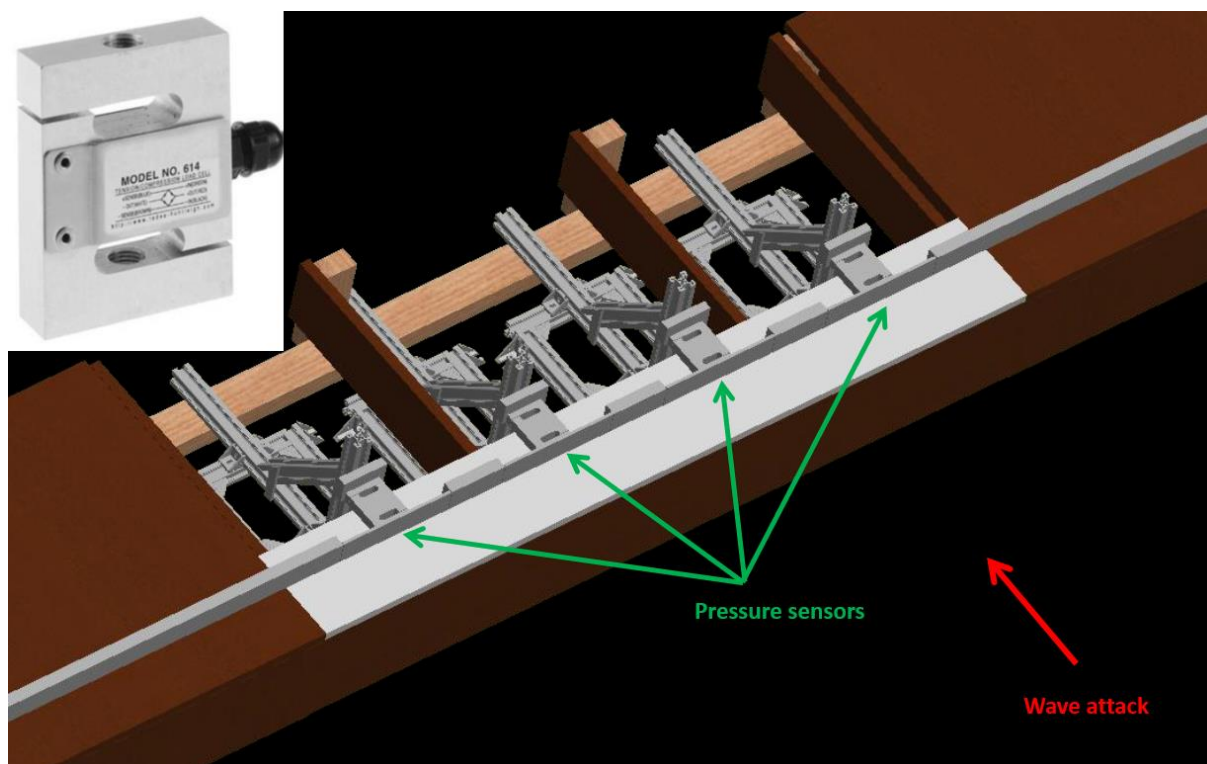
257 forces acting on the storm return wall (**Error! Reference source not found.** and). A minimal
 258 distance between the wave maker and the structure of two wave lengths was respected for all tests.

259 Three positions of the structure in the basin were foreseen. Firstly, the structure was mounted in the
 260 central down part of the basin for the 0° wave direction. Secondly, the structure was moved towards
 261 the down left corner to optimize the distance to the wave maker and to obtain the angle of 45° without
 262 changing the position of the wave paddle. Thirdly, the structure was moved for the 80° wave angle
 263 attack.



264

265 **Figure 4.** The structure used to investigate the force reduction (posterior view) (not to scale).



266

267 **Figure 5.** Force sensors were installed location as designed.

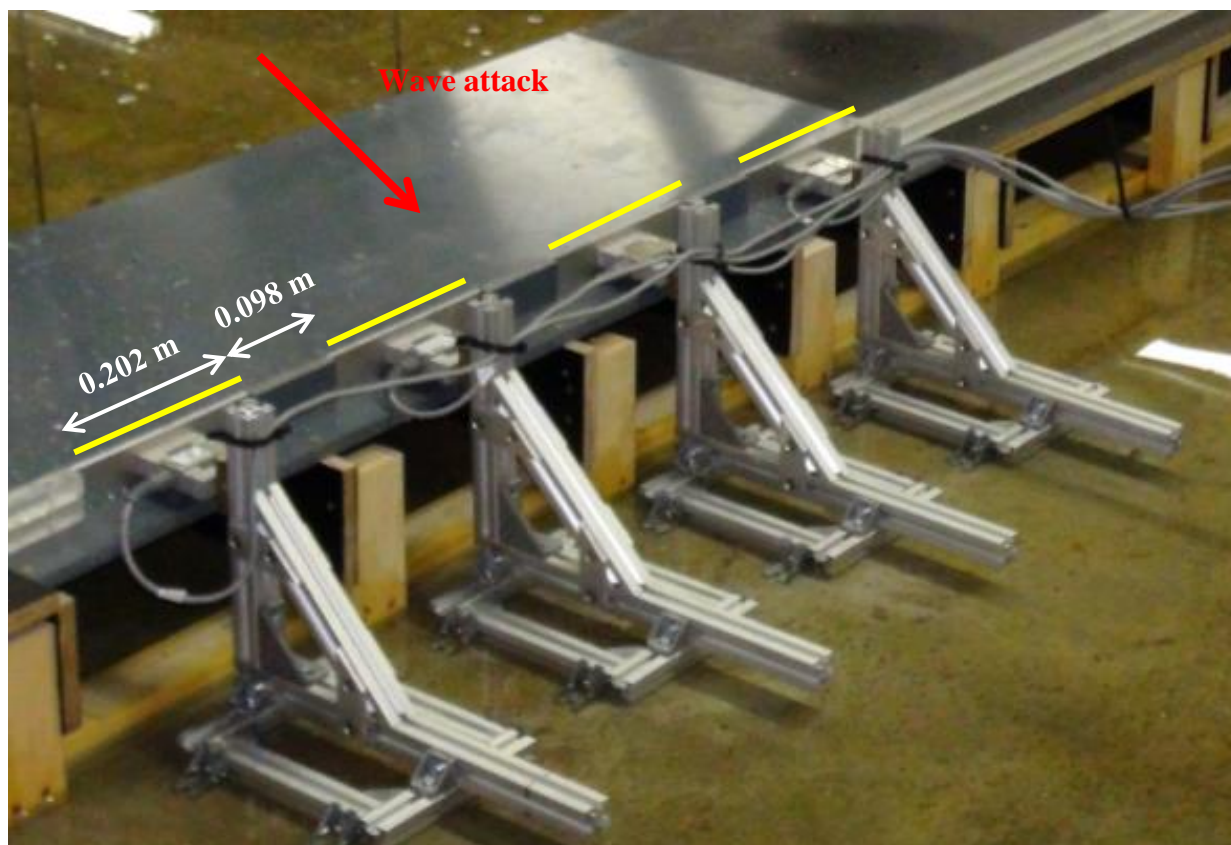
268 3.2.1. Instrumentation

269 The wave gauges were installed in a similar position as for the overtopping model and four force
 270 sensors were installed to measure the forces acting on the storm return wall at a frequency of 1 kHz
 271 (**Error! Reference source not found.** and **Error! Reference source not found.**). A number of 44
 272 successful tests were performed (**Error! Reference source not found.**).

274

Table 4. Summary of the test conditions for the force reduction.

	Total number of tests			44
Wave directions	Wave height (H_{m0})	Wave period (T_p)	Crest freeboard (R_c)	Storm return wall position
0°, 45°, 80°	1.04 to 4.54 m	10.2 to 12.9 s	0 to 3.0 m	0 to 25 m



275

276

Figure 6. The part of the structure where the force sensors were installed (detailed picture).

277 **4. Results**

278 *4.1. Overtopping reduction*

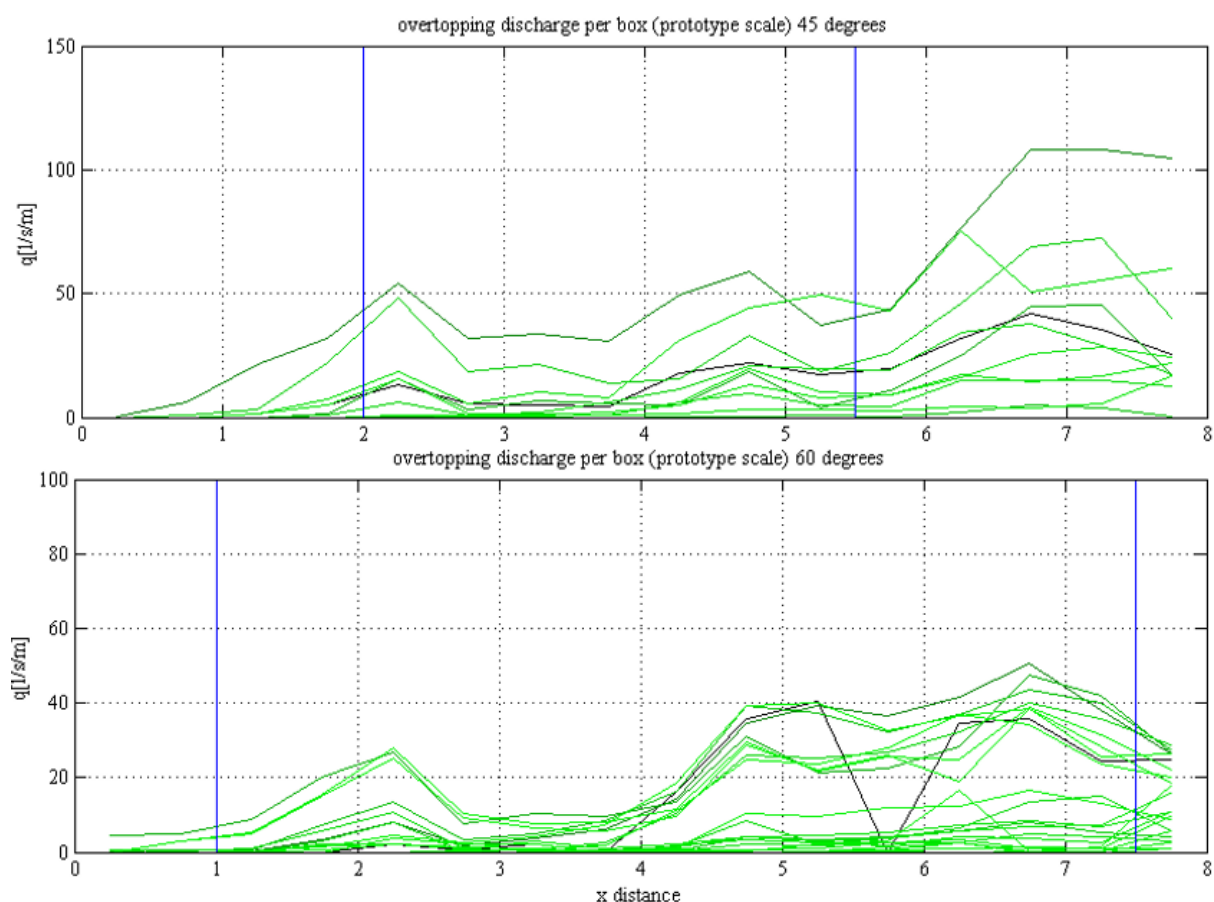
279 The measured average wave overtopping has been compared with the predicted values using
 280 the existing formulas. A reduction coefficient for each direction has been assessed using the FHR tests
 281 results: both mean value and standard deviation of the reduction coefficient have been calculated.
 282 The distribution of overtopping along the overtopping boxes was analyzed and correlated to the total
 283 wave height measured at the toe of the structure. For the analyses of the overtopping reduction due
 284 to the obliqueness, only tests without crest berm or with very short crest berm (5 m in prototype)
 285 have been considered. The influence of long crest berms has been analyzed afterwards.

286 Physical model test results included in the CLASH database [11] similar to the test from the
 287 present study have been used for comparison. In detail:

- 288 - Sloping dike: only CLASH data with slope between 1:4 and 1:2 with gentle or no foreshore
 289 have been considered;
- 290 - Vertical quay: only tests with gentle or without foreshore have been considered.

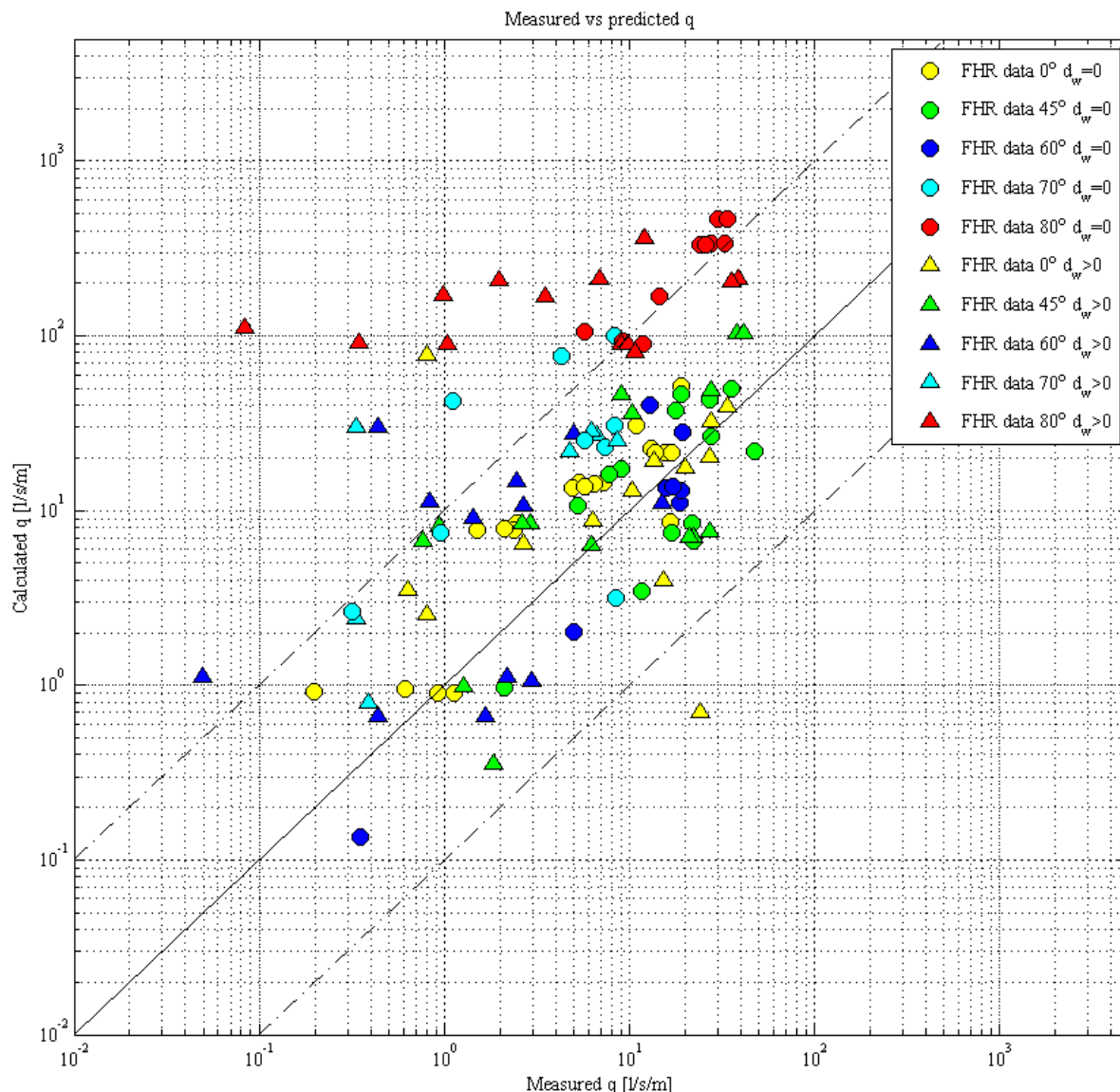
291 **4.1.1. Vertical quay wall**

292 The results of the tests indicate a clear decrease in the overtopping volumes with the increase of
 293 the wave angle. An increase of the overtopping volumes along the structure was observed for all
 294 cases, except for the perpendicular waves. In **Error! Reference source not found.** an example is
 295 shown and the horizontal axis represent the quay extension, from 0 to 8.0 m, where the 0 is taken in
 296 the corner of the structure closest to the wave paddle. Each line plotted in every figure represents the
 297 results from one model test. The distribution of the wave overtopping along the vertical quay is
 298 generally consistent with the distribution of the total wave height at the toe.



299
 300 **Figure 7.** Overtopping discharge per box along the vertical quay for directions 45° and 60°.

301 **Error! Reference source not found.** shows the results of the FHR tests in a graph with the
 302 measured discharges plotted against the predicted ones, expressed in l/s/m (prototype scale). The
 303 plotted data include cases without a crest berm (distance of the wall from the edge of the quay, d_w ,
 304 equal to 0 m) and with a crest berm (d_w larger than 0 m). The dash-dot lines indicate a prediction of
 305 10 times larger and smaller with respect to the central line (ratio predicted/measured equal to 1:1).
 306 The formula overestimates the overtopping discharge for the 70° and 80° directions, while for the 0°,
 307 45° and 60° directions results are in reasonable agreement or within the above mentioned range.



308

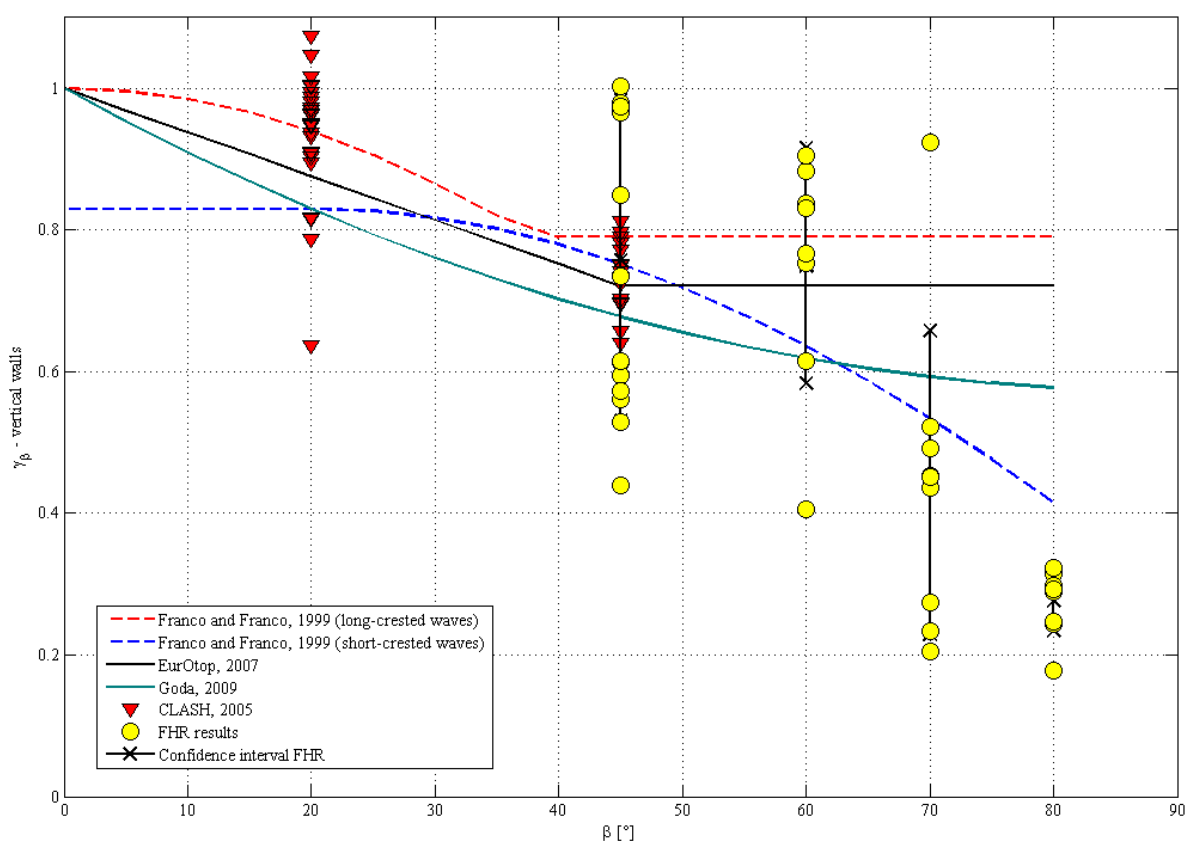
309 **Figure 8.** Quay wall: predicted [2] vs. measured overtopping discharges. The circles indicate the cases
 310 without berm crest (d_w=0), the triangles indicate the cases where a berm crest is present (d_w>0).

311 The effects of the obliqueness on the overtopping discharge have been evaluated calculating the
 312 reduction coefficient of each case, starting from equation (14), as follows:

313

$$\gamma_{\beta} = -2.6 \frac{R_c}{H_{m0}} \frac{1}{\ln\left(\frac{q}{0.04 \sqrt{gH_{m0}^3}}\right)} \quad (14)$$

314 The calculation has been performed both for the FHR data and for the selected CLASH data.
 315 **Error! Reference source not found.** shows the variation of the reduction coefficient with the wave
 316 angle. The existing formulations were analysed to calculate the reduction coefficient as function of
 317 the wave angle. Despite the scattering of the results (similar scatter can also be noticed in Goda, 2009)
 318 a certain trend can be identified.



319

320 **Figure 9.** Quay wall: variation of reduction coefficient with wave angle, comparison to existing
 321 formulas.

322 The tests clearly show that the overtopping discharge is inversely proportional to the wave
 323 angle: the larger the wave angle, the smaller the wave overtopping. Different formulas propose
 324 constant values for the overtopping volumes for waves larger than 37° (long crested waves, [16]), or
 325 45° [2]. Franco and Franco formula [16] for short-crested waves seems to be the closest to FHR results,
 326 although the FHR tests were conducted using just long-crested waves. However, the differences due
 327 to the “short-crestedness” lie within the scattering of the formula, similar to previous studies [17].
 328 Franco and Franco [16] stated that the directional spreading might allow reducing the freeboard with
 329 30% in respect to cases with only long-crested waves.

330 The results of the experiments indicate that no formula, among those previously proposed
 331 predicts accurately the overtopping reduction. However, it is preferable to use the formula proposed
 332 by Goda [1] for large angles due to two main reasons:

- 333 a) the correction coefficient represents an upper limit (safe approach) for the present cases with
 334 very oblique waves, although not excessively high as EurOtop [2];
- 335 b) the expression for γ_β is applicable up to 80°, meanwhile EurOtop [2]) indicates a constant
 336 value for wave angles larger than 45°.

337 The mean overtopping discharge is generally expressed by means of an exponential function as
 338 follows:

339
$$\frac{q}{\sqrt{gH_{m0}^3}} = A \exp\left(-B \frac{R_c}{H_{m0}\gamma_\beta}\right) \tag{15}$$

340 where:

- 341 • $A=0.040$ and $B=2.6$ in EurOtop [2];
- 342 • $A=0.033$ and $B=2.3$ in Goda [1];
- 343 • $A=0.116$ and $B=3.0$ in Franco and Franco [16].

344 Note that the reduction coefficient γ_β is a function of the A and B coefficients. The differences
345 between Goda [1] and EurOtop [2] can be considered negligible, because the values of A and B
346 coefficients are rather similar.

347 New values for the reduction coefficient are presented here based on the FHR data and it is
348 proposed to be used for similar conditions (Table 3). The resulting values, based on the FHR
349 measurements, including the standard deviation, can be summarized as follows:

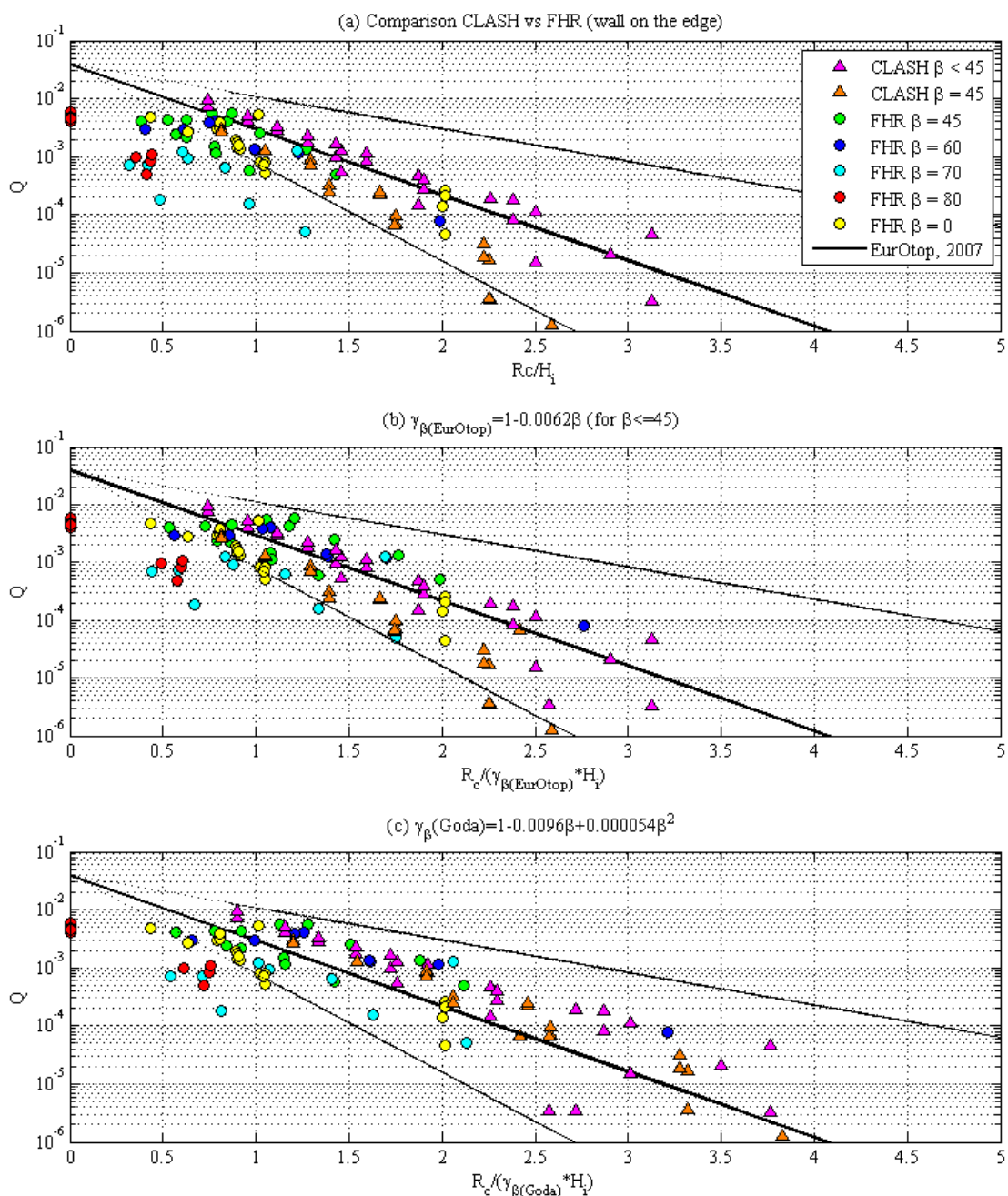
- 350 • $\gamma_\beta=0.76$ ($\sigma=0.23$), for $\beta=45^\circ$;
- 351 • $\gamma_\beta=0.75$ ($\sigma=0.17$), for $\beta=60^\circ$;
- 352 • $\gamma_\beta=0.44$ ($\sigma=0.21$), for $\beta=70^\circ$;
- 353 • $\gamma_\beta=0.28$ ($\sigma=0.04$), for $\beta=80^\circ$.

354 The calculated gamma value is the mean value for each wave angle. The mean values and
355 standard deviation values have been calculated for each wave angle starting from the results of γ_β
356 estimated for each single test. The confidence interval represented in **Error! Reference source not
357 found.** is calculated as $\pm\sigma$ with respect to the mean value. As general approach, the mean value of γ_β
358 has to be used for design purposes. It can be noticed that the difference in the reduction coefficient
359 between 0.72 (calculated value using EurOtop [2]) and 0.28 might cause a difference in the calculated
360 discharge of at least 1 order of magnitude (10 times) in the selected data range.

361 **Error! Reference source not found.** shows the FHR data, the CLASH data and the EurOtop
362 predictions in term of non-dimensional discharge $Q=q/(g \cdot H_{m0^3})^{0.5}$. Only the FHR cases with the wall
363 on the edge of the quay are plotted in order to avoid misinterpretations due to the effects of the width
364 of the crest berm. Three different plots are shown in **Error! Reference source not found.:**

- 365 a) the values of Q are plotted against the non-dimensional freeboard R_c/H_i ;
- 366 b) the values of Q are plotted against the non-dimensional freeboard $R_c/H_i\gamma_\beta$ (EurOtop), where
367 γ_β (EurOtop) is the correction coefficient calculated using the EurOtop (2007) formula;
- 368 c) the values of Q are plotted against the non-dimensional freeboard $R_c/H_i\gamma_\beta$ (Goda), where γ_β
369 (Goda) is the correction coefficient calculated using the Goda [1] formula;

370 The use of Goda [1] formula is improving the wave overtopping prediction in case of oblique wave
371 attack with respect to the EurOtop [2] formula. In most of the cases, especially for very oblique angles,
372 the EurOtop formula seems to overestimate the overtopping, while using Goda correction factors the
373 results are spread around the formula prediction and only few of them are still overestimated.



374

375

Figure 10. CLASH and FHR (wall on the edge of the quay) data vs EurOtop [2] predictions.

376

377

378

379

380

381

382

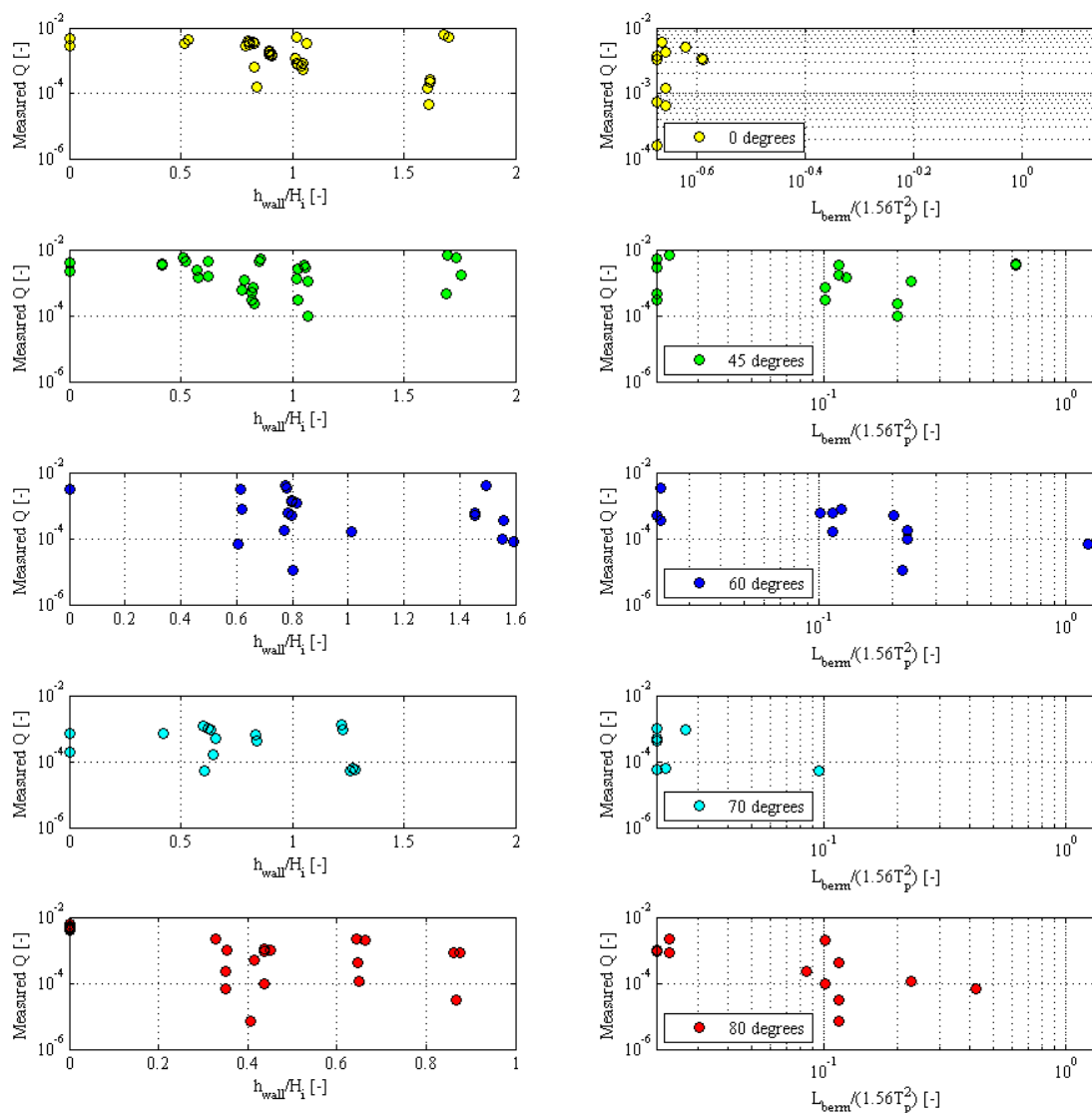
383

384

385

The analysis on the berm length effects (distance between the seaward edge of the quay and the storm wall) and on the wall height has been carried out. **Error! Reference source not found.** shows the non-dimensional overtopping discharge in function of two different non-dimensional parameters: (i) the ratio between the wall height and the incident wave height, (ii) the ratio between the berm length and $1.56T_p^2$ that can be assumed as the wave length in deep water conditions. The combination of obliqueness, wall height and berm length makes it challenging to have a clear view of the phenomena occurring at the structure. Despite the rather wide data scatter, there are clear differences between short or no berm layouts and wide berm layouts. A dependence on the berm length can be detected, the overtopping is reducing when the ratio of the berm length over the wave length is increasing and this trend is clearer for larger wave angles. The waves are travelling at the

386 dike crest before approaching the storm wall and it is expected that the waves refract on the berm
 387 and therefore approaching the wall with less obliqueness, but still not perpendicular. Then, the
 388 distance travelled by the waves to reach the wall is larger for larger angles, so the amount of energy
 389 dissipated on the crest might be larger. The configurations without berm and with short berm length,
 390 5 m in prototype, show a similar behaviour leading to larger overtopping discharge than the
 391 configurations with wider berms (25 m and 50 m in prototype).



392

393

394

Figure 11. Non-dimensional discharge vs relative wall height and relative berm length (quay layout).

395 4.1.2. Sloping dike

396

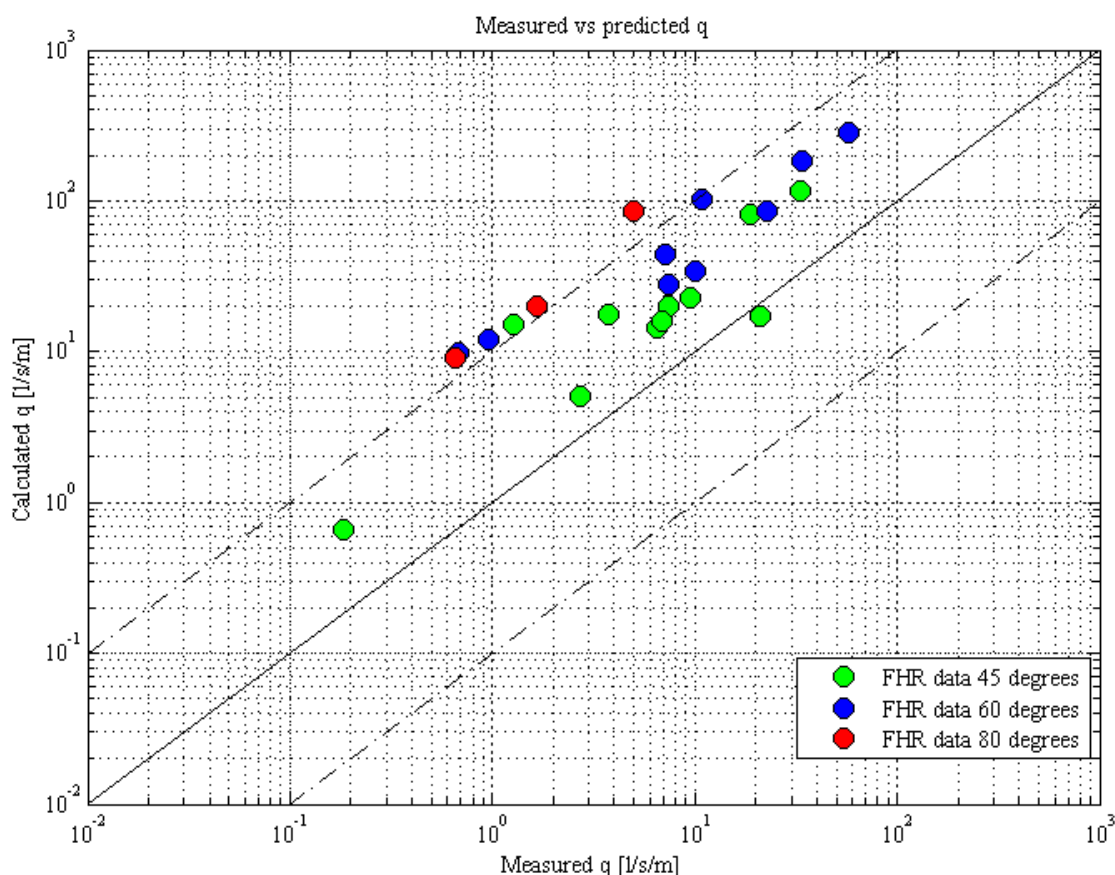
397

398

399

400

The results of the tests for a sloping dike are similar with those for a vertical quay, indicating the same decrease in the overtopping volumes with the increase of the wave angle. The measured overtopping discharges for FHR data are plotted in **Error! Reference source not found.** against the values predicted using equations (3) and (4) [1]. As noticed in the previous cases, the formula seems to overestimate the overtopping discharge for very oblique wave attacks.



401

402

Figure 12. Dike: predicted (EurOtop, 2007) vs. measured overtopping discharges.

403

The effects of the obliqueness on the overtopping discharge have been evaluated calculating the reduction coefficient of each case starting from equation (3) as follows:

404

405

$$\gamma_{\beta} = -2.6 \frac{R_c}{H_{m0} \gamma_{prom,v}} \frac{1}{\ln\left(\frac{q}{0.2 \sqrt{gH_{m0}^3}}\right)} \quad (16)$$

406

The calculation has been performed both for the FHR data and for the selected CLASH data.

407

Three different dataset have been selected from CLASH (for only non-breaking wave conditions):

408

- Dataset 030 [18]: 1:2 slope with 1:20 foreshore;

409

- Dataset 220 [19]: 1:2.5 slope with 1:1000 foreshore;

410

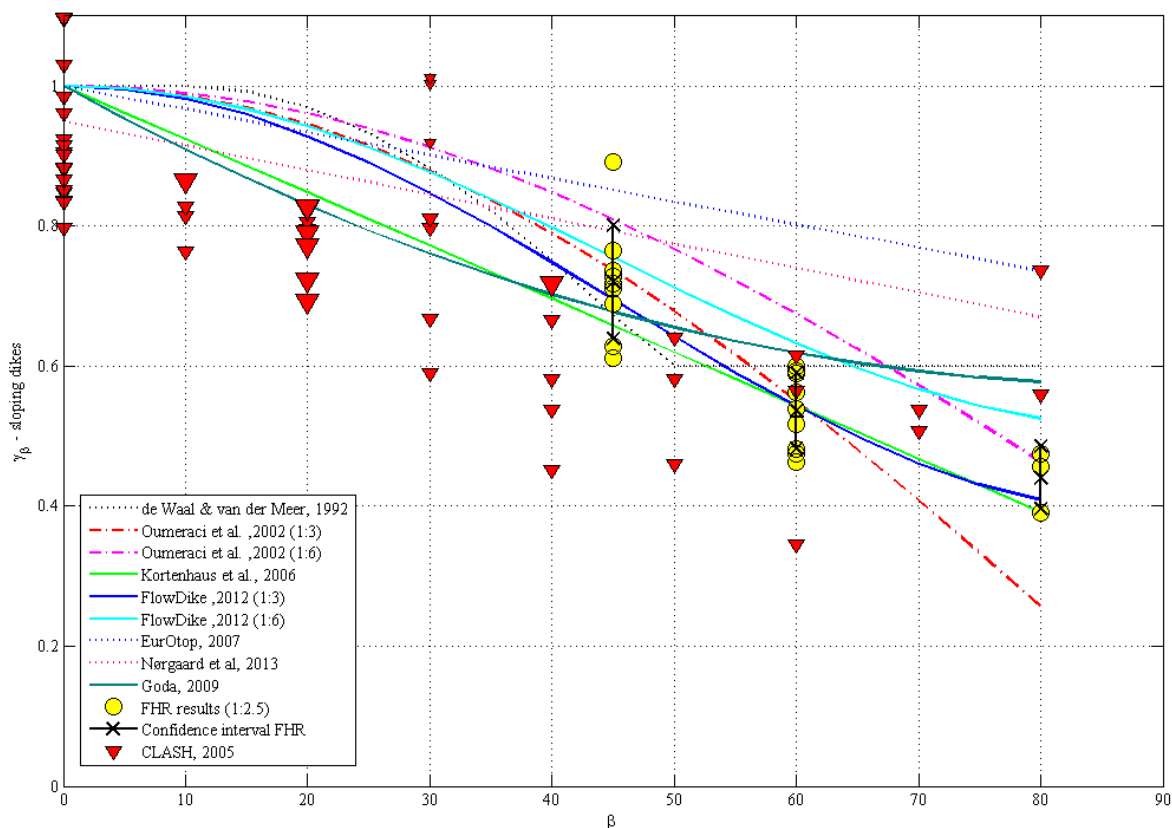
- Dataset 222 [19]: it includes data for 1:2.5 and 1:4 slope with 1:1000 foreshore.

411

Error! Reference source not found. shows the variation of the reduction coefficient with the wave angle. The CLASH data are labelled as red triangles whose size is proportional to the slope (e.g. 1:2 larger size than 1:4). Several proposed formulations have been analysed to calculate the reduction coefficient as function of the wave angle. The formulas predictions and the confidence interval for the FHR data are also plotted.

414

415



416
417
418

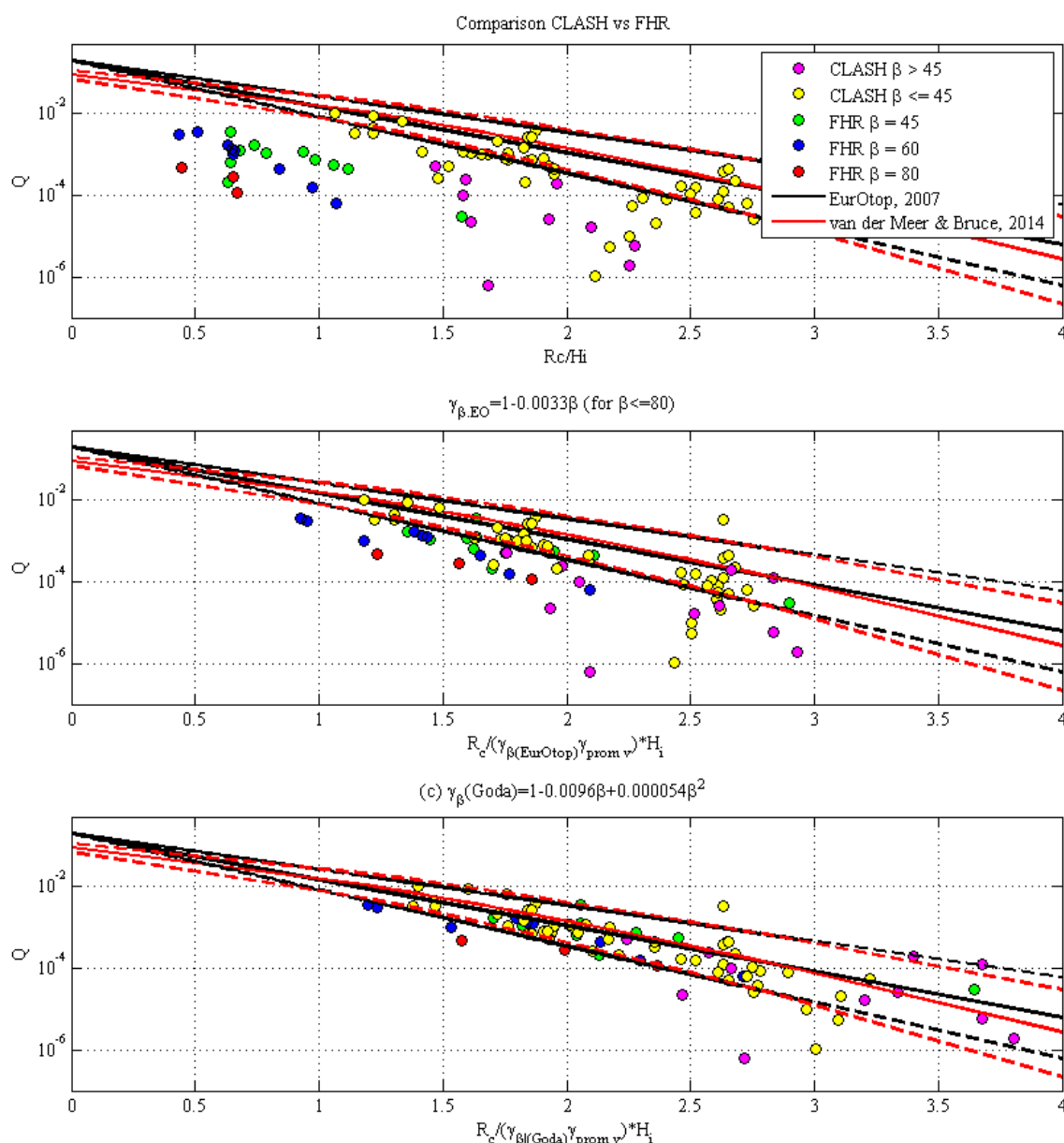
Figure 13. Sloping dike: variation of reduction coefficient with wave angle; comparison with existing formulas.

419 The results display a scattered distribution, but similar scatters can be observed in other studies
420 performed in similar conditions [1, 20]. However, a certain trend is visible and the reduction of the
421 FHR data are in agreement with the reduction of the CLASH data. **Error! Reference source not found.**
422 shows the FHR data, the CLASH data and the EurOtop predictions. Three different plots are
423 depicted:

- 424 a) the values of Q are plotted against the non-dimensional freeboard R_c/H_i ;
- 425 b) the values of Q are plotted against the non-dimensional freeboard $R_c/H_i \gamma_{\beta(EurOtop)} \gamma_{prom_v}$, where
426 $\gamma_{\beta(EurOtop)}$ is the correction coefficient calculated using the EurOtop [2] formula and γ_{prom_v} is
427 the reduction coefficient calculated by means of Van Doorslaer [9];
- 428 c) the values of Q are plotted against the non-dimensional freeboard $R_c/H_i \gamma_{\beta(Goda)} \gamma_{prom_v}$, where
429 $\gamma_{\beta(Goda)}$ is the correction coefficient calculated using the Goda [1] formula.

430 Similar improvement of the wave overtopping prediction as in the case of a vertical quay when
431 Goda formula is used over EurOtop formula can be observed for sloping dike cases.

432 The influence of the geometrical layout is not easily detected due to interference between three
433 involved parameters: obliqueness, wall height and berm length. However, the existence of the wall
434 significantly reduces the wave overtopping for all cases. Position of the storm return wall is also
435 important, larger berms leading to a decrease in the overtopping volumes.



436

437

Figure 14. FHR and CLASH data vs formula predictions.

438

4.2. Force reduction

439

The measured forces are plotted in **Error! Reference source not found.** (in prototype scale both vertical quay and sloping dike) in function of the incident significant wave height. The colors indicate the wave angle, respectively red for 0°, yellow for 45° and blue for 80°. The different shapes indicate the results from each different load cell: this allows underlining that, despite the waves are long-crested, the forces exerted along the structure have a certain variability. As expected, the forces increase with the wave height. It is clear that the 0° cases result in larger forces than the 45° case and the 80° cases have the lowest forces. For the same wave height, the very oblique cases present in average a value of the wave

447

force that is almost half of the perpendicular case.

448 The data were analyzed to define an analytical expression for the reduction factor. This
 449 coefficient is the ratio between the force due to an oblique wave attack over the force in case of
 450 perpendicular waves reaching the structure. The reduction factor expresses how much the data from
 451 cases with oblique attack should be corrected to be in line with a 0° case that present the same
 452 hydraulics boundary conditions (except from the obliqueness).

453 Two different expressions, respectively for quay walls and dikes, have been found:

$$454 \quad \gamma_{quay} = \frac{F_{quay,\beta>0}}{F_{quay,\beta=0}} = 0.5 \cdot (1 + \cos\beta) \quad (17)$$

$$455 \quad \gamma_{dyke} = \frac{F_{dyke,\beta>0}}{F_{dyke,\beta=0}} = \exp(-0.007\beta) \quad (18)$$

456 where β is the wave direction relative to the structure (perpendicular wave direction = 0°, angle
 457 expressed in degrees). The expression for quay walls is corresponding to the formula for caisson
 458 breakwaters proposed by Goda [21].

459 The two expressions for the reduction factor could certainly be improved if additional data with
 460 other wave angles than 45° and 80° would be available. However, the new proposed expressions can
 461 already be considered as a significant improvement in the prediction. In **Error! Reference source not**
 462 **found.** the measured wave forces are plotted in function of the relative freeboard. Four pictures are
 463 reported, two for the dike cases and two for the quay wall cases. In detail:

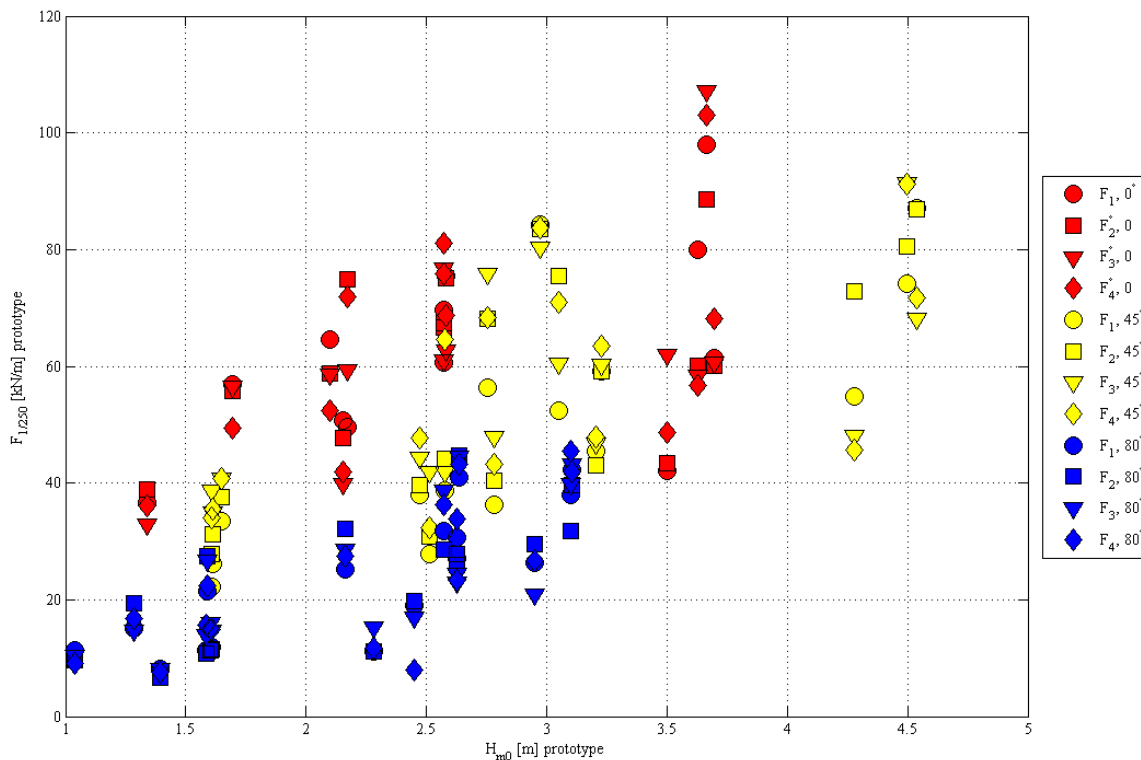
- 464 a) measured wave force on the storm wall for the quay wall layout;
- 465 b) measured wave force on the storm wall for the sea dike layout;
- 466 c) measured wave force on the storm wall for the quay wall layout, including the correction
 467 with the proposed reduction factor for wave obliqueness;
- 468 d) measured wave force on the storm wall for the sea dike layout, including the correction with
 469 the proposed reduction factor for wave obliqueness.

470 The scatter in the wave forces is significantly reduced if the wave force is corrected using the
 471 reduction factor proposed above. This improvement has also been quantified by the relative standard
 472 deviation for each case ($\mu' = \mu/\sigma$):

- a) $\mu'=7.9\%$; b) $\mu'=7.0\%$;
- c) $\mu'=8.8\%$; d) $\mu'=4.7\%$.

473 The analysis of the overall results finally suggests that, in case of very oblique wave attack
 474 (obliqueness between 70° and 80°) the expected force on the storm wall range between 55% to 65% of
 475 the value in case of perpendicular wave attack.

476

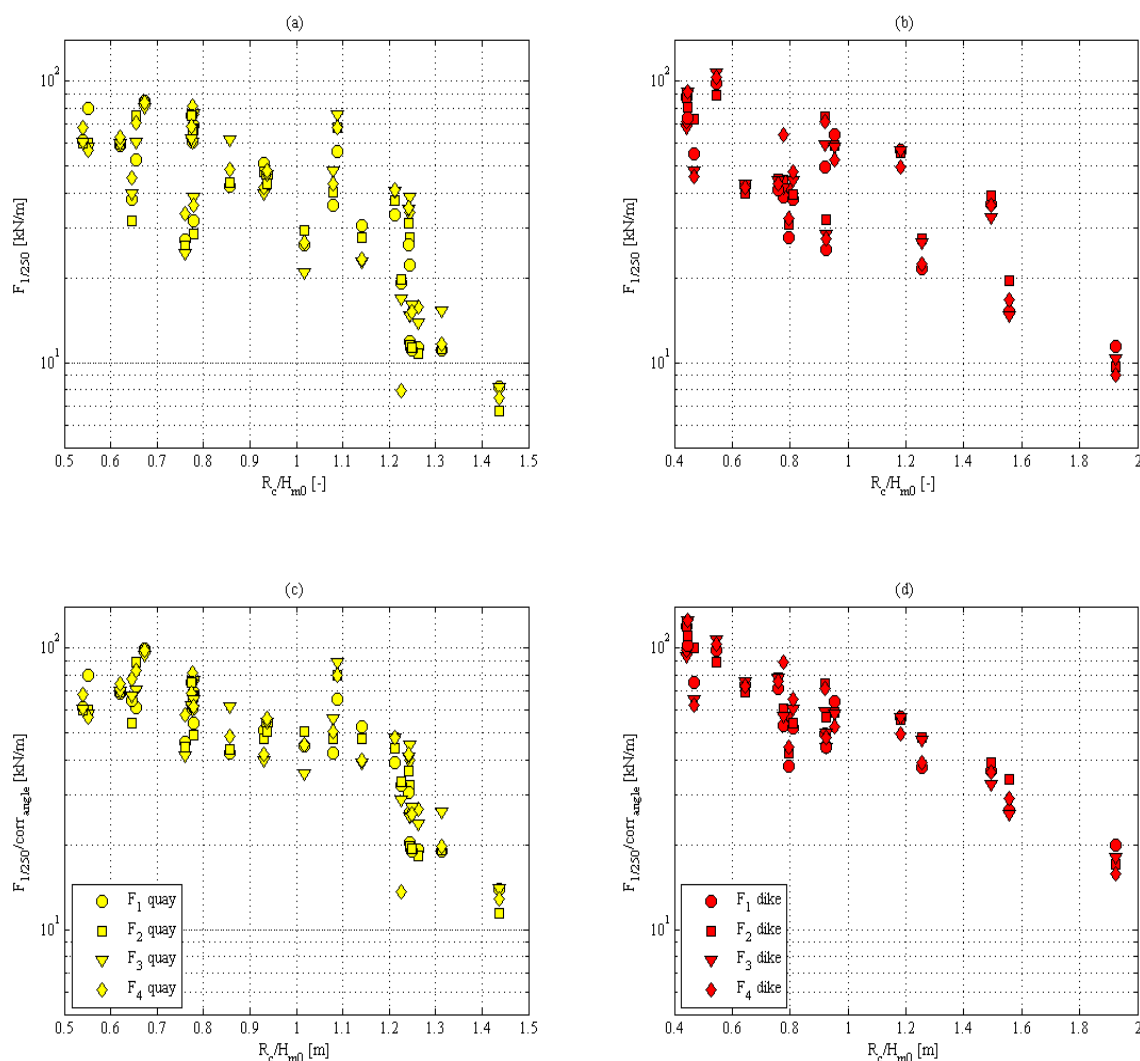


477

478

479

Figure 15. Dependence of the wave forces on the incident wave height for different wave obliqueness.



480

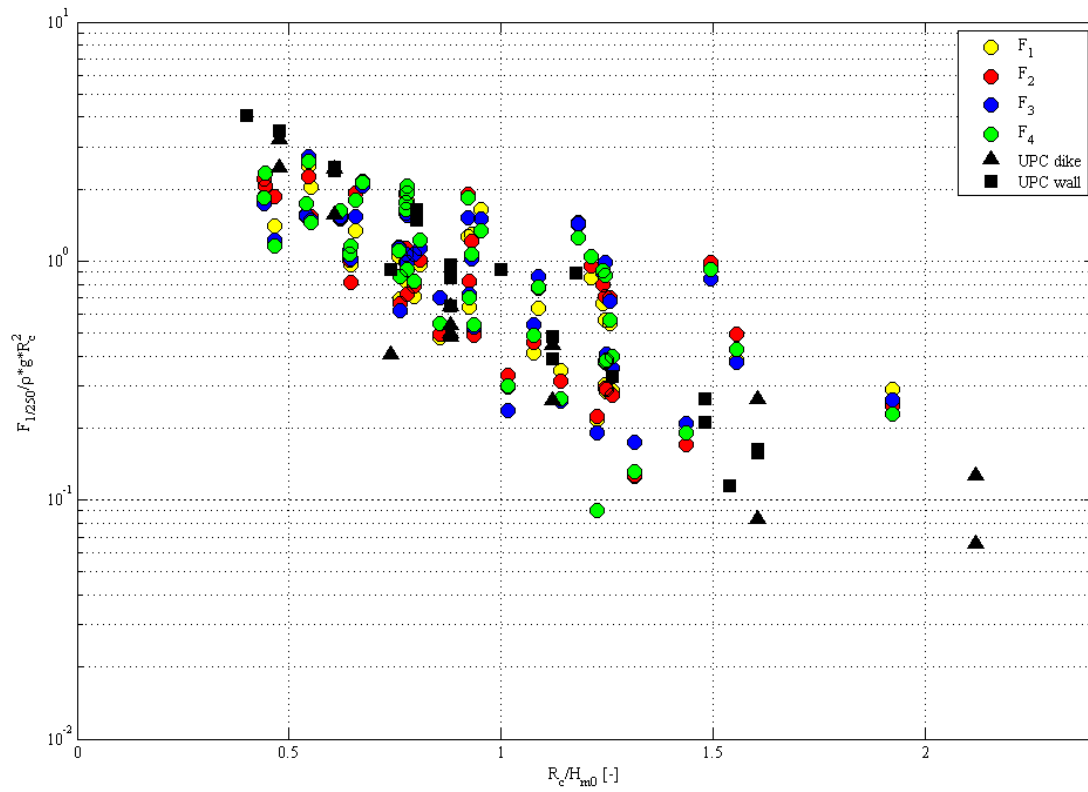
481 **Figure 16.** Dependence of the wave force on the relative freeboard with and without reduction factor
 482 (a & c: quay wall, b & d: dike).

483 The results of the FHR tests are compared to predictions of the formula proposed by Van
 484 Doorslaer et al. [10] for sea dikes, regardless of its range of applicability (e.g. wall position and wall
 485 height are different). **Error! Reference source not found.** depicts the variation of the non-dimensional
 486 quantity $F_{1250}/\rho g R_c^2$ as function of the relative freeboard, both for FHR and UPC results. A common
 487 trend between the two experimental datasets can be noticed, despite of a certain scatter in the FHR
 488 results, mainly due to the different wave angles.

489 Equation (13) has been applied to the FHR and UPC data: only FHR cases with 0° have been
 490 initially considered for comparison, as the UPC data refer to perpendicular wave attack. The results
 491 of the are plotted in **Error! Reference source not found.**. Generally, equation (13) underestimates the
 492 force for FHR cases probably due to different wall height between UPC data and FHR data,
 493 respectively 1.2 m and 2.0 m (in prototype scale). Higher walls would lead to smaller overtopping
 494 rates and bigger reflection exerted by the storm wall with consequent higher forces on the same wall.

495 In the next step equation (13) has been applied to all FHR data and the results are reported in
 496 **Error! Reference source not found.** both without and with application of the reduction factors
 497 (equations (17) and (18)) for wave obliqueness. Without correction, the prediction show a large

498 scatter, while the application of the reduction factor reduces significantly the scatter and improves
 499 the predictions. Nevertheless, the estimated forces are still slightly smaller than the measured ones
 500 and it can be concluded that the correction applied to take into account the wave obliqueness
 501 improves the predicted forces.



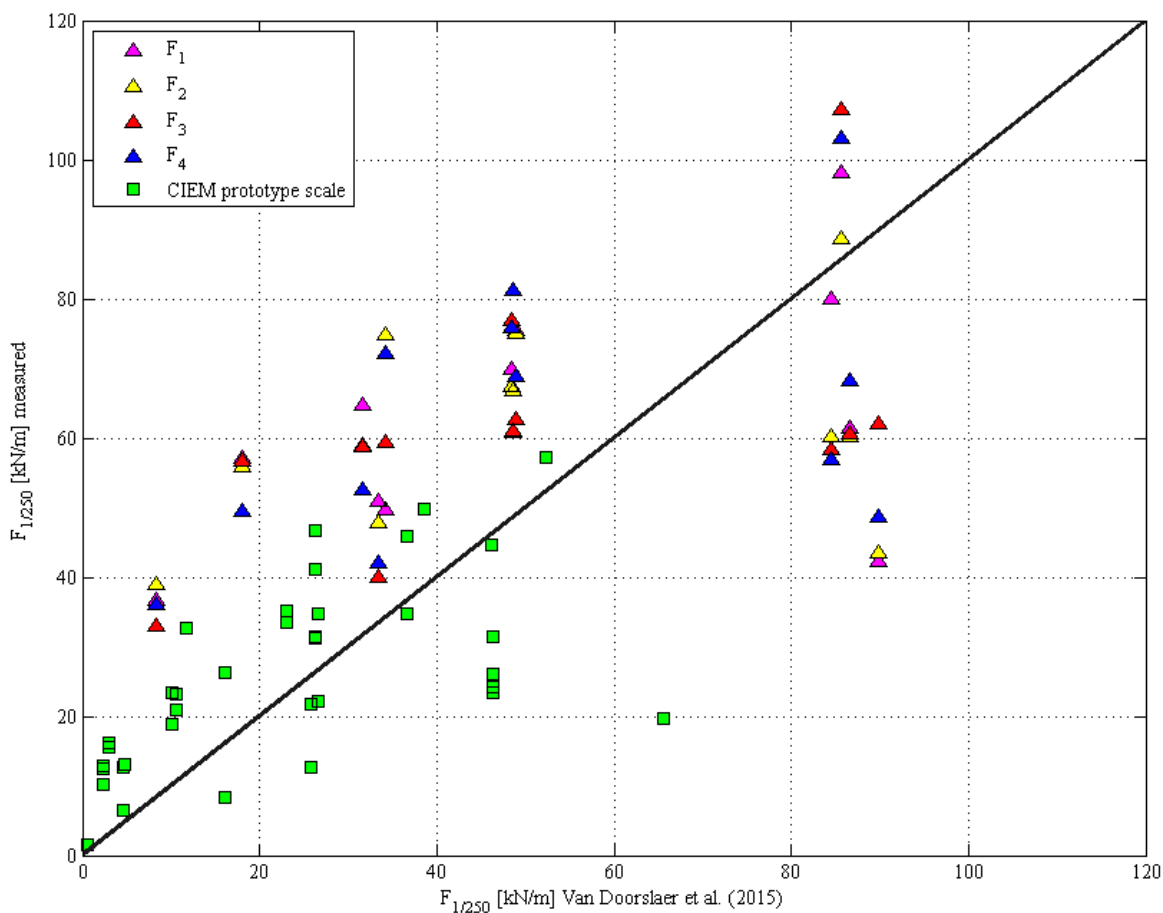
502

503

504

Figure 17. Dependence of the non-dimensional wave forces on the relative freeboard and comparison with data from UPC [10].

505

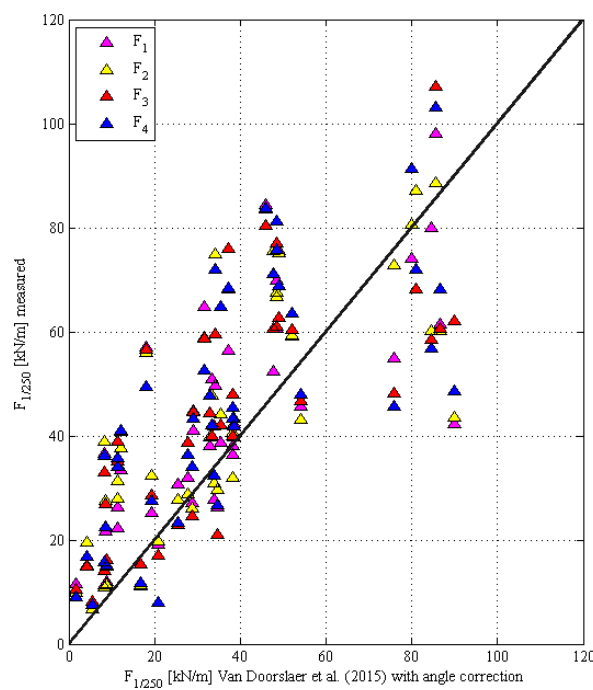
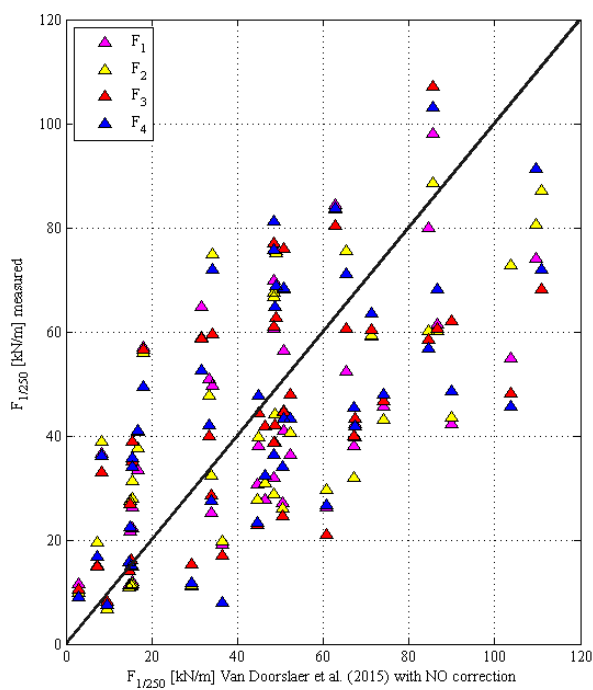


506

507

508

Figure 18. Measured forces versus Van Doorslaer et al. [10] predictions for FHR 0° cases and UPC cases.



509

510

511

Figure 19. Application of Van Doorslaer et al. [10] formula with and without reduction factor for wave obliqueness.

512 5. Conclusions

513 The present study describes the setup and the results of physical model tests carried out at FHR
514 on wave overtopping generated by perpendicular and very oblique waves, based on the generic
515 configurations and conditions at Belgian harbors. A set of different wave angles has been tested: for
516 a vertical quay layout: 0°, 45°, 60°, 70° and 80° and for the dike layout: 45°, 60° and 80° have been
517 investigated.

518 The reduction in overtopping discharge has been quantified and the results have been compared
519 with similar tests in the CLASH database [11] and with predictions by several semi-empirical
520 formulas and correction factors from literature.

521 The influences of the storm wall height and the crest berm width have been investigated together
522 with the effect of wave obliqueness.

523 The analysis of the results for the vertical quay and sloping dyke layouts leads to the following
524 conclusions:

- 525 1. The EurOtop formula [2] generally overestimates the overtopping discharge for large wave
526 obliqueness.
- 527 2. The values of the reduction factor γ_β calculated for the vertical quay layout are equal to 0.76,
528 0.75, 0.44 and 0.28 respectively for 45°, 60°, 70° and 80°.
- 529 3. The values of the reduction factor γ_β calculated for the sloping dike layout are equal to 0.72,
530 0.54 and 0.44 respectively for 45°, 60° and 80°.
- 531 4. A rather large scatter is present in the results similar to the results presented in previous
532 studies [1].
- 533 5. The expression of γ_β presented by Goda [1] is finally proposed as a good compromise
534 between accuracy (in comparison with physical model results) and a certain safety in the
535 design of the storm walls.
- 536 6. The high obliqueness combined with long berms on the crest (comparable with the wave
537 length) leads to very low or zero overtopping discharge.
- 538 7. The berm length (ranging from 0 to 50 m) has a larger influence on the overtopping
539 discharge than the wall height (ranging from 1 to 2 m).

540 Tests have been performed to identify the wave force impact reducing due to wave obliqueness
541 both for sea dyke and for quay wall layouts. The wall height was 2.0 m (in prototype scale) and it was
542 located at three different distances from the seaward edge of the main structure (berm).

543 The results indicate that for high wave obliqueness the force reduction in case of very oblique
544 waves is 0.55 - 0.65 times the wave forces for similar wave conditions, but for perpendicular wave
545 attack. Two reduction factors have been defined, respectively for the sea dyke and the vertical quay
546 wall layout as presented in equations (17) and (18). Finally, the formula of Van Doorslaer et al. [10]
547 has been applied, confirming that the use of the above mentioned reduction factors reduces the
548 uncertainties in the wave force predictions due to the effects of the wave obliqueness.

549 Due to the limited amount of available data, the relationship between wave obliqueness and
550 other variables such as wall position has not been analyzed in the present study. Further studies on
551 wave forces on storm walls on top of sea dykes or quay walls should take into account this reduction
552 if the waves are approaching the structure with an angle larger than 45°.

553 **Author Contributions:** Sebastian Dan: Conceptualization, methodology, resources, data curation and analysis,
554 writing—original draft preparation, supervision, project administration. Corrado Altomare: Conceptualization,
555 methodology, software, validation, data analysis, investigation, data curation, writing—review and editing,

556 visualization. Tomohiro Suzuki: Software, validation, formal analysis, investigation, writing—review and
557 editing. Tim Spiesschaert: Physical test execution, wave basin set up, data collection and analysis. Toon
558 Verwaest: writing—review and editing, project administration, funding acquisition.

559 **Acknowledgments:** The authors are grateful to Agentschap voor Maritieme Dienstverlening en Kust (MDK) –
560 Coastal Division, Belgium for financing this study, to Thomas Lykke Andersen, University of Aalborg and to
561 Marc Willems, Flanders Hydraulics Research, for their valuable suggestions regarding wave measuring and
562 processing and the experiment set up. Corrado Altomare acknowledges funding from the European Union’s
563 Horizon 2020 research and innovation programme under the Marie Skłodowska-Curie grant agreement
564 No.:792370.

565 **Conflicts of Interest:** The authors declare no conflict of interest. The funders had no role in the design of the
566 study; in the collection, analyses, or interpretation of data; in the writing of the manuscript, or in the decision to
567 publish the results.

568 References

- 569 1. Goda, Y. Derivation of unified wave overtopping formulas for seawalls with smooth, impermeable surfaces
570 based on selected CLASH datasets. *Coast. Eng.*, 2009, vol. 56, pp 385-399.
- 571 2. *European Overtopping Manual for the Assessment of Wave Overtopping (EurOtop)*. Eds. Pullen t., Allsop N.W.H.,
572 Kortenhaus A., Schüttrumpf H., van der Meer J.W., 2007, www.overtopping-manual.com .
- 573 3. van der Meer, Jentsje & Allsop, William & Bruce, Tom & Rouck, Julien & Kortenhaus, Andreas & Pullen,
574 T. & Schüttrumpf, Holger & Troch, Peter & Zanuttigh, Barbara. *EurOtop: Manual on wave overtopping of sea
575 defences and related structures - An overtopping manual largely based on European research, but for worldwide
576 application (2nd edition)*, 2016.
- 577 4. De Waal, J.P.; van der Meer, J.W. Wave run-up and overtopping on coastal structures. *ASCE, proc. 23rd
578 ICCE*, Venice, Italy, 1992, pp. 1758-1771.
- 579 5. Kortenhaus, A.; Geeraerts, J.; Hassan, R. Wave run-up and overtopping of sea dikes with and without
580 stilling wave tank under 3D wave attack (DIKE-3D), *Final Report*, Braunschweig, Germany, 2006.
- 581 6. Chen, W., Van Gent, M.R.A., Warmink, J.J., Hulscher, S.J.M.H. The influence of a berm and roughness on
582 the wave overtopping at dikes. *Coast. Eng.*, 2020, Vol. 156 <https://doi.org/10.1016/j.coastaleng.2019.103613>.
- 583 7. van Gent, M.R.A. Influence of oblique wave attack on wave overtopping at smooth and rough dikes with
584 a berm. *Coast. Eng.*, 2020, Vol. 160.
- 585 8. Van der Meer, J.W.; Bruce, T. New physical insights and design formulas on wave overtopping at sloping
586 and vertical structures. *ASCE Journal of Waterway, Port, Coastal & Ocean Engineering*, ASCE, 2014, ISSN 0733-
587 950X/04014025(18).
- 588 9. Van Doorslaer, K.; De Rouck, J.; Audenaert J.; Duquet V. Crest modifications to reduce wave overtopping
589 of non-breaking waves over a smooth dike slope. *Coast. Eng.*, 2015, Vol. 101, pp. 69-88.
- 590 10. Van Doorslaer, K., Romano, A., Bellotti, G., Altomare, C., Cáceres, I., De Rouck, J., Franco, L., van der Meer,
591 J. Force measurements on storm walls due to overtopping waves: a middle-scale model experiment.
592 *Proceedings of International Conference on Coastal Structures, Boston, 2015*.
- 593 11. Verhaeghe, H.; van der Meer, J.W.; Steendam, G.J. *Database on wave overtopping at coastal structures, CLASH
594 report, Workpackage 2, 2004*, Ghent University, Belgium.
- 595 12. Hughes, S.A. (1993). *Physical Models and Laboratory Techniques in Coastal Engineering*. Vol.7, World
596 Scientific Publishing, Singapore, 568 pp.
- 597 13. Schüttrumpf, H.; Oumeraci, H. (2005). Layer thicknesses and velocities of wave overtopping flow at
598 seadikes. *Coast. Eng.*, 2005, Vol. 52, pp. 473-495 <http://dx.doi.org/10.1016/j.coastaleng.2005.02.002>
- 599 14. WaveLab 3 homepage Aalborg University. 2012, <http://www.hydrosoft.civil.aau.dk/wavelab/>
- 600 15. Hashimoto, N.; Kobune, K. (1987). "Directional spectrum estimation from a Bayesian approach". *Proc. 21st
601 Conference on Coastal Engineering, 1987, Vol. 1*, pp 62-76, Costa del Sol-Malaga, Spain
- 602 16. Franco, C.; Franco, L. Overtopping formulas for caissons breakwaters with nonbreaking 3D waves. *Journal
603 of Waterways, Port, Coastal and Ocean Engineering*, 1999, pp 98-107.
- 604 17. Vanneste, D.; Verwaest, T.; Mostaert, F. *Overslagberekening Loodswezenplein Nieuwpoort: Versie 2.0. WL
605 Adviezen, 15_005, 2015*, Waterbouwkundig Laboratorium (Flanders Hydraulics Research) Antwerpen,
606 België, in Dutch.

- 607 18. Owen, M.W. Design of seawalls allowing for wave overtopping. *Hydraulics Research, Wallingford, Report No.*
608 *EX 924, UK, 1980.*
- 609 19. Van der Meer, J.W. en de Waal, J.P. Invloed van scheve golfval en richtingspreiding op galfoploop en
610 overslag. "Influence of oblique wave attack and directional spreading on wave run-up and overtopping".
611 *Delft Hydraulics Report on model investigation, H638, 1990, in Dutch.*
- 612 20. Bornschein, A.; Pohl, R.; Wolf, V.; Schüttrumpf, H.; Scheres, B.; Troch, P.; Riha, J.; Spano, M.; van der Meer,
613 J. Wave run-up and wave overtopping under very oblique wave attack (CORNERDIKE-Project). *Proc. of*
614 *the HYDRALAB IV Joint User Meeting, Lisbon, July 2014.*
- 615 21. Goda, Y. New wave pressure formulae for composite breakwater, *Proc. 14th Int. Conf. Coastal Engineering,*
616 *1974, Copenhagen, ASCE, pp.1702-1720.*

617



© 2020 by the authors. Submitted for possible open access publication under the terms and conditions of the Creative Commons Attribution (CC BY) license (<http://creativecommons.org/licenses/by/4.0/>).

618